DOKUZ EYLÜL UNIVERSITY
GRADUATE SCHOOL OF NATURAL AND APPLIED SCIENCES

DEVELOPMENT OF A HEAT TRANSFER MODEL FOR WASTE-WATER HEAT RECOVERY SYSTEM

by
İlayda Farahnaz YILMAZ

October, 2020
İZMİR

DEVELOPMENT OF A HEAT TRANSFER MODEL FOR WASTE-WATER HEAT RECOVERY SYSTEM

A Thesis Submitted to the
Graduate School of Natural and Applied Sciences of Dokuz Eylül University In Partial Fulfillment of the Requirements for the Degree of Master of Science in Mechanical Engineering, Thermodynamics Program

by
İlayda Farahnaz YILMAZ

October, 2020
İZMİR

M.Sc THESIS EXAMINATION RESULT FORM

We have read the thesis entitled **“DEVELOPMENT OF A HEAT TRANSFER MODEL FOR WASTE-WATER HEAT RECOVERY SYSTEM”** completed by **İLAYDA FARAHNAZ YILMAZ** under supervision of **ASSOC. PROF. MEHMET AKİF EZAN** and we certify that in our opinion it is fully adequate, in scope and in quality, as a thesis for the degree of Master of Science.

Assoc. Prof. Dr. Mehmet Akif EZAN

Supervisor

Prof.Dr. Aytunç EREK

Assoc.Prof.Dr. Orhan EKREN

Prof. Dr. Özgür ÖZÇELİK
Director
Graduate School of Natural and Applied Sciences

ACKNOWLEDGEMENT

I would like to offer my gratitude to my advisor, Assoc. Prof. Mehmet Akif EZAN, who did not withhold his support and valuable feedback from the first day I applied for the master education until my last day. I would like to thank him for sharing his extensive and vast knowledge with me and for his share in the success of my thesis. I will always be grateful for working with such an open-minded, skilled advisor.

I would also like to thank Asst. Prof. Jean DUQUETTE from Carleton University, Canada, for his informative and helpful consultations and his valuable contributions to this work.

I would like to thank Hüseyin ÇOBAN for being honest with me and spend his time on making many brainstorms.

Finally, I would like to thank my family for supporting me and being understanding when I need it.

İlayda Farahnaz YILMAZ

DEVELOPMENT OF A HEAT TRANSFER MODEL FOR WASTE-WATER HEAT RECOVERY SYSTEM

ABSTRACT

Condensers are an essential part of a vapor-compression heat pump cycle, which is commonly used for residential waste-water heat recovery systems. Heat exchangers with the multi-phase flow, such as the condenser, are one of the most complicated elements of a heat pump cycle. This study is mainly focused on condensers and their behavior in the case of simultaneous heat rejection and condensation. Rejected heat from the condenser has a significant potential for energy recovery and can be later used to supply heat to another source such as waste-water of which heat will be recovered or tap water. For the storage of this recovered energy, phase change materials are used, and they are aimed to store the rejected heat from the condensing refrigerant. In the mathematical model, the energy equation for the double pipe condenser with R134a refrigerant is resolved in the enthalpy form. The upwind scheme is used to discretize the governing equations. Different empirical equations for the heat transfer coefficient from literature are compared. After verification of the condenser model with similar work from literature, paraffin as phase change material (PCM) is added to the system. The thermal energy that is released during the condensation is stored by PCM. Later on, this recovered and stored energy is aimed to be used in another process. For the modeled condenser, temperature distribution and vapor quality are given with time. For the PCM results, temperature variations with time are evaluated. According to the results, the condenser model with and without PCM can be used to predict the thermal behavior of a condenser, and the developed model shows good consistency with the literature.

Keywords: Condenser, two-phase flow, numerical model, phase change material

ATIK SU ISI GERİ KAZANIM SİSTEMİ İÇİN ISI TRANSFERİ MODELİ GELİŞTİRİLMESİ

ÖZ

Kondenserler, evsel atık su ısı geri kazanım sistemlerinde yaygın olarak kullanılan buhar sıkıştırmalı ısı pompası çevriminin önemli bir parçasıdır. Kondenser gibi çok fazlı akışa sahip ısı değiştiricileri, bir ısı pompası çevriminin en karmaşık unsurlarından biridir. Bu tezde, esas olarak kondenserlere ve eşzamanlı ısı salınımı ve yoğuşma durumundaki davranışlarına odaklanılmıştır. Kondenserden atılan ısı, enerji geri kazanımı için önemli bir potansiyele sahiptir ve daha sonra ısısı geri kazanılacak bir atık su veya musluk suyu gibi başka bir kaynağa ısı sağlamak için kullanılabilir. Geri kazanılan bu enerjinin depolanması için faz değiştirici malzemeler kullanılmaktadır ve yoğuşan soğutucu akışkandan aktarılan ısının depolanması amaçlanmaktadır. Geliştirilen matematiksel modelde, R134a soğutucu akışkanlı çift borulu kondenserin enerji denklemi, entalpi formunda çözülmüştür. Korunum denklemlerinin ayrıklaştırılmasında Upwind şeması kullanılmıştır. Literatürden farklı ısı transfer katsayısı korelasyonları karşılaştırılmıştır. Kondenser modeli literatürdeki benzer bir çalışma ile doğrulandıktan sonra sisteme faz değişim malzemesi (PCM) olarak parafin eklenmiştir. Yoğuşma sırasında açığa çıkan ısı enerjisi PCM tarafından depolanmaktadır ve daha sonra geri kazanılan ve depolanan bu enerjinin başka bir proseste kullanılması amaçlanmaktadır. Modellenen kondenser için zamana bağlı sıcaklık dağılımı ve buhar kalitesi verilmiştir. PCM sonuçları için sıcaklık değişimi zamana bağlı olarak verilmiştir. Elde edilen sonuçlara göre, PCM'li ve PCM'siz kondenser modeli, bir kondenderin termal davranışını tahmin etmek için kullanılabilir ve geliştirilen model, literatür ile iyi bir tutarlılık göstermektedir.

Anahtar Kelimeler: Kondenser, iki fazlı akış, sayısal model, faz değişim malzemesi

CONTENTS

Page

LIST OF FIGURES

LIST OF TABLES

CHAPTER ONE
INTRODUCTION

In the last decade, the tremendous growth of industrialization and population with fossil energy depletion leads to energy shortage and environmental pollution. Thus, developing methods that permit to utilize energy sources more efficiently and economically gained significant importance and expected more actively developed. Alternative solutions such as renewables and improved energy usage methods by minimizing the loss and energy recovery are now occupying a prominently important place in the energy area.

Energy recovery is one of the trending solutions, and the main idea is to recuperate the wasted, rejected energy, and re-utilize it for a system in need (Ramadan, Lemenand, & Khaled, 2016). A heat recovery application into a system can provide energy saving up to 80% (Nyers, 2016). According to the International Energy Agency (Bor, Ferreira, & Kiss, 2015), heat as an energy usage represents 47% of the worldwide total energy consumption. Heat is necessary for many applications, and thereby it should be used, stored, and recovered efficiently to be more advantageous in both an environmental and economical way.

In domestic applications, both air conditioning and hot water needs are mostly provided by the heat pump mechanism. Heat pumps can be supplied with renewable energy and are widely used in apartments, offices, or hospitals. There has been considerable progress, especially in recent years, and in this respect, heat pumps can offer an environmentally friendly solution (Hepbasli, 2014). However, there is still a significant amount of waste heat from the cycle, and it would impact the environment severely if a recovering solution is not developed.

In a residential living area, there is generally two dominant use of energy, which are air conditioning and hot water use (Chen & Lee, 2010). A large amount of produced heat, which is around 40% in the domestic buildings in an average city, is wasted to the sewage. This waste heat can be used in a place that requires energy in the system, and it will also reduce the thermal pollution in the surroundings before it is released. There are a couple of methods that are used to recover waste heat from a residential place. For example, recovering the heat of condenser in the cycle of the heat pump is a favorable option and drew attention as a way for saving energy in recent years (Qiu, Li, & Xu, 2019). In a space cooling system, this method can be one of the most economical solutions for the conservation of energy (Chen & Lee, 2010). In that kind of system, rejected heat from the condenser can be transferred to a source such as water or phase change material, which can later be used for energy supply. The other commonly applied method is recovering heat from waste-water in houses to preheat the supply tap water. Each of these methods can be used to lower energy consumption and increase efficiency. Such heat recovery systems will provide both environmental and economic benefits.

Each of the methods mentioned above uses storage media such as water or phase change material or directly heat the water, air, or another source, for energy recovery. Energy demand in a residential building does not match with the energy source or recovery in general. Energy storage provides an option of energy reservoir to eliminate this mismatch, and energy needs would be fulfilled any time when there is a demand (Sari & Kaygusuz, 2001). For the thermal energy storage method, the sensible heating of water is widely used (Gu, Wang, Liu, & Ma, 2004). However, water requires a large volume, and its capacity for energy usage is low even though its good heat transfer characteristics and economic advantage. One of the highly preferred methods for energy storage is latent heat storage using phase change material (PCM) (Zalba, Marin, Cabeza, & Mehling, 2003). Due to their high energy storage density compared to sensible heat storage, the required volume and weight are smaller in the latent heat storage method. The latent heat storage method is particularly attractive since the late 70s. PCMs can change phase at almost constant temperature and stores the heat of fusion at that temperature (Agyenim, Hewitt, Eames, & Smyth, 2010).

In this thesis, the primary focus is on a condenser that operates with waste-water from a residential area. As an element of the residential heat pump cycle, the condenser releases heat while its operation, and instead of sending this waste heat to the sewage, the developed model first stores the waste heat through PCM and transfers to the waste-water when the regeneration of storage material came up. Later on, additionally heated waste-water, which was previously hotter than tap water, could be used to pre-heat the tap water. However, directly recovering wastewater heat is not studied in this work, but only a literature review and the potential of this method are given.

In order to understand the condenser properly, different solution methods and numerical models are investigated. Since there is a phase transition from vapor to liquid phase inside the condenser, flow mechanisms and heat transfer become more complicated. Using an appropriate approach for the condenser solution is essential to take forward this problem of energy storage and recovery. For this reason, a general numerical method is developed to predict the thermal behavior of condenser and use it in later scenarios within the scope of this work.

1.1 Literature Review

In the following sub-sections, the literature on waste-water heat recovery units, the modeling of multi-phase flow, and the heat exchanger models with phase change materials are summarized.

1.1.1 Waste-Water Heat Recovery Systems and Heat Exchangers

Baek, Shin, & Yoon. (2005) designed and analyzed a vapor compression heat pump system with wastewater usage from the sauna of a hotel. The system uses off-peak electricity during nighttime, and wastewater is stored in a tank as a heat source, and heated tap water is also stored in a hot water storage tank. For the numerical simulations, the TRNSYS software is used. They simulated the system for different seasons and the hours of one day, and they have obtained the COP values, temperatures in both tanks, and condenser outlet temperature. According to their results, the designed system can provide 100% of hot water demand and can supply over 90% of the hot water load except for the weekend in the winter season.

Chao, Yiqiang, Yang, Shiming, & Xinlei (2012) built an experimental setup that is based on a heat pump system using waste-water from a common bathroom discharge. Various operating conditions are measured to evaluate the energetic effect of waste-water heat recovery. In the developed system, waste-water from a SPA center bathroom is collected in a storage tank, and an evaporator of the heat pump is placed inside the tank. The refrigerant flows inside the evaporator and receives heat from the waste-water, and then refrigerant completes the heat pump cycle through the compressor and condenser. After the evaporator chills waste-water, it is discharged to the sewage. As a result, they evaluated the temperature variations in waste-water, hot water, and refrigerant against time. They have also analyzed COP variation for an entire month in order to assess the fouling effect on the system, and they made an economic comparison with conventional heating methods for 15 years. In conclusion, they have found that the circulation of waste-water inside the tank can improve the performance, and using this system can be financially advantageous. However, periodical cleaning should always be applied as the bio-fouling reduces system performance.

Chen et al. (2013) modeled a heat pump water heater for bathing. In this system, there is a regenerator and evaporator which uses hot waste-water from the shower. R134a is chosen as a refrigerant, and each of the elements is calculated using thermodynamic models. The system is analyzed in both steady and transient state, and the effects of condenser inlet temperature, condensing, and evaporating temperature on COP and input power are evaluated. For the two-phase flows, the local heat transfer coefficient is assumed to be linear to the vapor fraction. According to the results obtained, the COP of the system increase with the decreasing condenser inlet temperature. Besides, the temperature difference between wastewater and refrigerant at the condenser inlet is not higher than 2°C, which means the proposed system can fully use waste-water energy and largely reduces the waste heat discharge.

Mcnabola & Shields (2013) carried out experimental and numerical analyses of a horizontal drain-water heat recovery system for domestic showers. For the experiments, a PVC wastewater pipe with thinner copper water supply pipe, which is wrapped around it, is used, and temperature distribution inside the pipes is obtained. For the numerical solution, a commercial computational fluid dynamic software package CFX is used. Heat transfer is modeled using the thermal energy heat transfer model, and for the fluid flow inside the cold-water pipe, the *k*-epsilon turbulence model is used. In the drainpipe, a free surface multiphase flow model is used. According to the results, the designed system could operate at a satisfactory level of efficiency despite a couple of modifications are need to be done for practical use. In addition, the economic analysis shows that it is viable to invest.

Nyers (2016) designed a heat recovery system that uses a plate heat exchanger between two heat pump cycles with a lower and higher temperature range. In the first stage, heat recovery from washing machine wastewater is made by the plate heat exchanger in which clean cold water flows from one end, and hot waste-water flows on the other end. The second stage of the heat recovery has occurred in the first heat pump. Clean water and waste-water flow inside the evaporator of the system, and heat is transferred to the clean water. Finally, on the third stage, the clean water which flows inside the condenser of the first heat pump flows through the condenser of the second heat pump, and similarly, the wastewater from the first heat pump evaporator flows inside the evaporator of a second heat pump. Heated water is gathered inside a tank. For the mathematical solution of the system, basic thermodynamic equations are used, and COP values and energy efficiency are obtained. According to the results, 83-85% of the energy demand for water heating can be supplied by the developed recovery system.

Ramadan et al. (2016) developed a calculation procedure for drain heat recovery systems. The procedure requires the water flow rate and the temperature from the supply tank and the hot return water temperature from the residence. According to the input values, recovered heat and power consumption can be calculated. For this calculation, the experimental setup is used, and measured input data is obtained. Experiments showed that the system could be used to increase the temperature of the cold supply water, and the efficiency of the recovery system decrease with the cold inlet temperature.

Ekren, Araz, Hepbasli, Biyik, & Gunerhan (2016) experimentally analyzed the performance of a wastewater heat pump system, which was installed in Turkey. The refrigerant used in the system was R134a, and the system is worked in the wastewater-air mode for cooling and heating. Results depicted that using waste-water heat recovery can provide efficiency up to 44% in both heating and cooling. Also, the total saving amounts for the year are 675 kWh and $81. According to their study, wastewater source has higher energy potential than air source.

1.1.2 Numerical Modeling of Multiphase Heat Exchangers

Wang & Liao (1989) studied the transient response of the condensing flow in a horizontal double-pipe condenser to a sudden change of refrigerant mass flow rate. The study was both theoretical and experimental, of which results are compared with the theoretical method. For the experiments, a vapor compression cycle system is used. For the solution of condensing flow, two phases, two-fluid model, which takes account flow inertia and compressibility of vapor and tube wall thermal capacity, is used. In this model, vapor and liquid phases have different velocities. Governing equations are solved by an explicit finite difference scheme. Condensation is assumed to be fully annular, and there was a thermal equilibrium between phases. Fluid properties are taken from the Handbook of ASHRAE (1985) and JSME (1983). The frictional pressure gradient of two-phase flow is given by Lockhart-Martinelli correlation (Lockhart & Martinelli, 1949), and a two-phase multiplier by Soliman (1982) is used. For the convective heat transfer coefficient, correlation by Shah (1979) is solved.

Escanes et al. (1995) made a numerical simulation of the double pipe condenser and evaporator to obtain their fluid-dynamic and thermal behavior. Governing equations in one dimension and transient condition are solved iteratively for each of the control volumes. The model was based on two concentric pipes and the tube wall, which separates the refrigerant and heat transfer fluid flow. An implicit step-by-step method and an implicit central difference scheme are used for the numerical calculations of fluid flow and the tube wall, respectively. Required information for the convective heat transfer coefficient and friction factor is obtained by empirical equations. Two different criteria for the transition between phases are used, and the variation of temperature distribution in the pipes with time is given. The results are obtained for R134a and R12 in both condensing and evaporating flow.

Willatzen, Pettit, & Ploug-Sørensen (1998) presented a mathematical model that can be used for condensers and evaporators. All properties of refrigerant are defined using local conditions by a defined function. Mass and energy conservation equations are solved in one dimensional, and partial-differential equations are formulated depending on the fluid phase, which is divided into three regions as liquid, two-phase, and vapor. The developed model is later used in the second part of this study. Pettit, Willatzen, & Ploug-Sørensen (1998) simulated the thermal behavior of an evaporator, which is used in a vapor compression cycle. For the simulation of this evaporator model, moving from a nonlinear lumped moving boundary method is used. The results are given for over a wide range of operating conditions.

Garcia-Valladares, Perez-Segarra, Rigola, & Oliva (1998) worked on a one-dimensional condenser and evaporator model using two different algorithms; the pressure-based method, which they have defined SIMPLE-like, and the Step-by-Step implicit method, which basically calculates the outlet values from known inlet values. They used local thermophysical properties in governing equations. Results are given for different complex geometry configurations such as single and multiple pipes and both pure and mixed refrigerants. In the SIMPLE-like method, convective terms in equations are treated using first and higher-order numerical schemes such as central difference, SMART and QUICK. A comparison of four different numerical schemes using a different number of control volumes for condensation inside a single tube is given. According to their study, the QUICK or SMART scheme gives higher accuracy when compared to other numerical schemes. Additionally, they found that the Step-by-Step method gives a faster solution through the SIMPLE method is more general and applicable to complex geometries.

Garcia-Valladares, Perez-Segarra, & Rigola (2004) modeled a one-dimensional double-pipe condenser and evaporator in their study. Numerical work has been evaluated by an implicit step-by-step method using a central difference scheme for the discretization of the governing equations. For the transition between liquid and vapor states, two different approaches were compared. Results for the different aspect ratios with both pure and mixed refrigerants are given in transient conditions.

Rigola, Morale, Gustavo, & Segarra (2004) developed a one-dimensional, transient model for both condenser and evaporator. They have used a pressure-based SIMPLEC method by Patankar (1980) with special emphasis on the zones where phase transition takes place. For the condensing flow, Shah correlation (Shah, 1979) is used, and the model is verified through experimental work by Cavallini et al. (2001). For the evaporator, an experimental unit, which is the refrigerating equipment of the vapor compression cycle, is used for the validation. They have compared their numerical method with the step-by-step approach by Escanes, Pérez-Segarra, & Oliva (1995). As a result, the variation of pressure, convective heat transfer coefficient, and wall temperature depending on position are given. According to their results, step by step approach is similar by means of accuracy when compared to the SIMPLEC method, but it gives a faster solution.

Ruiz, Rigola, Pérez-Segarra, & García-Valladares (2009) studied both condensing and the evaporating flow inside a heat exchanger, which is solved with a semi-implicit numerical scheme for pressure linked equations. They have compared different numerical aspects and gave their results for the cases using different mass flux, pressure, and inlet temperature range. They presented a new criterion that improves the numerical method for the transition zones. In their study, solid domains as heat exchanger pipes are also solved. For the transient terms, the first-order backward differencing scheme is used. When solving the momentum equation, for the evaluation of the local shear stress, they have used a two-phase friction factor. For the condensing flow, they have preferred to use the correlation of Shah (1979). Numerical work has been compared with the experimental data from the literature. According to the results, even though the numerical model predicts the case with R22, it shows good agreement for the case with R134a.

Fayssal & Moukalled (2012) compared the effectiveness of four different numerical methods, which are finite-volume based, and they are applied to the condenser and evaporator model. Each method differs from each other by physical assumptions at the interphase between liquid and vapor regions and in the equation of vapor quality. For the comparison of numerical methods, an iterative solution algorithm that takes account of the local effects is developed. In the numerical solution, single-phase regions are not modeled, and only pure refrigerants are used. For the multi-phase flow, different morphologies are not adopted, but only an annular type of flow is considered for the whole phase transition process. Two of the methods have different vapor quality calculation. One of them uses energy conservation and calculates the distribution of vapor fraction utilizing enthalpy values. The second method, however, calculates the flow quality by mass conservation. Moreover, the other two methods are based on two different approaches for the heat transfer between different phases. The first of these methods assumes there is no heat transfer between vapor and liquid phases, which have exactly the same temperature. On the other hand, in the second method, vapor temperature and liquid temperature are not the same. Thus, there should be heat transfer between them. Thermodynamic properties are obtained using the NIST database by REPROP (REFPROP v.6.01. NIST). Parametric results for refrigerant type, pipe diameter, and mass flow rate are obtained. For the accuracy of this work, a comparison is made with experimental data.

1.1.3 PCM in Heat Exchangers

Gong & Mujumdar (1996) developed a numerical model of a heat exchanger with PCM using the finite element method by Galerkin (Zienkiewicz & Taylor, 1989) cited by Gong & Mujumdar (1996). For the numerical algorithm, overall energy balance is performed at each time step, and enthalpy stored in PCM is compared with thermal energy change in the heat transfer fluid, and temperature distribution is obtained through enthalpy change with time. Transient terms are discretized by a three-time level scheme. The main purpose of their work was to investigate the advantages of using multiple PCMs that have different melting temperatures. PCMs are placed on the outer pipe of the heat exchanger. For this study, PCM heat transfer is assumed to be conduction controlled, and the natural convection effect is neglected. According to their results, they have found that when multiple PCMs are used, the more uniform temperature distribution is formed in the heat exchanger and the outlet temperature of the heat transfer fluid became lower when compared to the case in which a single PCM is used. They have also investigated the effect of varying charge and discharge durations, and it is seen that when the charge or discharge cycle durations increase, enhancement from multiple PCMS decreases.

Long & Zhu (2008) studied the heat transfer model of PCM, which is based on pure conduction. For the calculation of temperature distribution and phase front location, a quasi-steady state method is used. Following numerical modeling, they have obtained experimental results from a heat pump with a PCM integrated water heater. During the off-peak time at night, PCM is melted with operating heat pump, and in the morning, melted PCM heats the water from approximately 30ºC to 50ºC. According to their study, this kind of water heater, which uses off-peak electricity, is more efficient than conventional electric-resistance water heater and need a smaller space than air-source heat pump water heater which has a tank. Average PCM temperature variation and power consumption are given. They also evaluated heat storage and release rate with time and solidification and melting front in the axial direction.

Rösler & Brüggeman (2011) modeled a shell and tube heat exchanger with paraffin PCM called RT42. The problem is solved using the enthalpy-porosity method with the function of liquid fraction. Enthalpy formulation using conservative equations on a fixed Eulerian grid is used for the conduction-driven phase change problem. In this method, latent heat depends on the PCM temperature is considered by a source term. Similarly, for the convection dominated phase transition, the same method is used, which accounts for the thermal properties using a mushy zone approach. For the simulations with convection, they have used a specially developed scheme for the enthalpy by Voller & Prakash (1987). In each iteration, flow quality is calculated and then used for the energy balance solution. They have defined the mushy region depending on flow quality. For the numerical solution, OpenFOAM is used, and the solution is validated through experimental work.

Maaraoui, Clodic, & Dalicieux (2012) developed a numerical model of PCM integrated condenser of air to air heat pump system. The condensing temperature of the condenser is used for the PCM melting at noon. Then, when the electricity peak load, the compressor is turned off, and the indoor air can be heated by transferring heat from the previously melted PCM. The numerical model is developed using finite volume, and for the phase transition, the Dumas approach is used. In this approach, the whole volume is considered as a single-phase depending on thermophysical properties. The energy equation in enthalpy form is solved for each volume, and the liquid fraction is introduced to describe the physical state of the fluid. For the results, a heat exchanger is simulated in discharging cases with different airflow regimes. They have found that capacity decreases with time. Thus, variable ventilation should be used to ensure constant capacity.

Parry, Eames, & Agyenim (2014) studied a numerical solution for one-, two-, and three-dimensional models of PCM heat exchanger using ANSYS Fluent. They have studied three different designs for the PCM applied to a heat exchanger. First, they developed a single tube model and then added fins for the heat transfer enhancement. The last design was a multi-tube heat exchanger with PCM. They have used experimental data from the literature for comparison of their numerical algorithm.

For the PCM, they have preferred organic PCM due to their good stability in terms of cyclic behavior. For the solution of connection during the melting process, they used an effective diffusivity method. Average PCM temperatures during both charging and discharging and transferred heat are obtained.

Hosseini, Rahimi, & Bahrampoury (2014) made both numerical and experimental study which focused on shell and tube heat exchanger with PCM. They have conducted numerous experiments for both charging and discharging processes to analyze the effects of increasing the inlet temperature of heat transfer fluid. For the numerical solution, iterative computations are conducted using finite volume single domain enthalpy formulation. They have found that increasing the inlet temperature of heat transfer fluid significantly affects the heat transfer rate and melting time of the PCM. The higher temperature values lead to the system efficiency becomes better.

Seddegh, Wang, & Henderson (2016) compared vertical and horizontal shell and tube heat exchanger with PCM. Numerical work is validated through literature. For the solution enthalpy method is used, and paraffin is used as the PCM. In each iteration, the liquid fraction is computed at each cell in the domain based on enthalpy balance. Additionally, the mushy zone between phases is modeled as a pseudo porous media in which porosity decreases from one to zero as the PCM solidifies. Ansys Fluent software is used for the transient solution, which uses the PRESTO scheme and second-order upwind scheme for the momentum and energy equation. According to their comparison, during charging, the horizontal heat exchanger convection has a significant effect on the upper part of PCM but less significant at the lower half. On the contrary, for the vertical placement, the convective heat transfer coefficient has the same effect in entire geometry. However, for the discharge, there is not any difference between horizontal and vertical heat exchangers. According to their results, horizontal placement shows better thermal performance when charging.

Qiao et al. (2018) applied PCM to a condenser of the vapor compression cycle. In this system, PCM operates as a thermal battery while storing the rejected heat of the condenser, and once the PCM is fully melted, the system is regenerated by a thermosyphon operation mode in which PCM releases its heat to the ambient. Paraffin PT37 is used as PCM. According to their study, once the PCM is completely melted, it makes condenser pressure and temperature go higher, which leads to the degradation of performance. Hence, PCM regeneration is obligatory.

1.1.4 Condensing Heat Recovery

Gu et al. (2004) stated that low-temperature hot water could be generated by recovering heat from air conditioning systems. In this study, both sensible and condensing heat is recovered by adding two accumulators after compressor discharge and also the outlet of the condenser. Paraffin was PCM, which is stated compatible with air conditioning systems is used in accumulators. PCM with a lower melting temperature is placed in the accumulator, which is after the compressor, and the other PCM with a higher melting temperature is placed in the accumulator after the condenser. Sensible heat and latent heat are stored in accumulators 1 and 2, respectively. Accumulator 2 is only used when the water demand is reached at some specified level. Thermodynamic calculation by enthalpy difference is conducted, and the system is analyzed by varying condensing temperatures.

Chen & Lee (2010) combined a space cooling and hot water pre-heating system which uses the rejected heat from the condenser. In his study, it is aimed to preheat tap water by utilizing the heat from the condenser during summer. Daily cooling and hot water demand are evaluated during both weekdays and weekends for different seasons.

Zhang, Yu, Yu, & Lin (2011) combined condensing heat recovery and latent heat storage using PCM in his study. Two different air conditioner systems are built up and experimentally investigated. In one of the systems, an additional container filled with paraffin as PCM is involved. In the system with the container, a refrigerant with high temperature and pressure values from the compressor passed through the PCM container before entering the air-cooled condenser, and the excessive heat before condensation is stored in the container where cold water flows through it when the hot water is needed. According to the comparison of with and without PCM container, cooling capacity and compressor power are increased, and the condensing temperature is decreased in the system with the container.

Qiu et al. (2019) studied a condensing heat recovery system in which a heat recovery heat exchanger and a hot water tank are placed between the compressor and air-cooled condenser. Simple thermodynamic models are used to obtain the operating behavior of these elements and also calculate the efficiency of this developed system. An experimental unit is used for both heating and cooling modes. According to their results, an 84% COP increase can be obtained in condensing heat recovery mode.

1.2 Objectives and Contributions of the Thesis

The major objective of this thesis and its contributions to the literature are as follows;

- To develop a numerical algorithm which can be used for the two-phase flow simulation of condensers in both steady-state and transient conditions,
- To predict the thermal behavior of the condenser,
- To implement a developed condenser algorithm to an energy storage system.

1.3 Content of the Thesis

Following chapter; chapter 2 deals with the numerical model of the condenser in both steady and transient states and represents the results for different flow parameters such as mass fluxes, diameter ratios, and refrigerants.

In Chapter 3, paraffin type PCM is implemented to the outer pipe of double pipe condenser, and the energy storage problem is analyzed for changing melting and condensation temperatures, PCM thicknesses, and refrigerant mass fluxes.

In the final part of this work, wastewater flows as soon as the system needs regeneration in order to continue to operate efficiently.

To specify a road map of each problem, after the mathematical model properties are given, the numerical method which is used in the problem will be mentioned. Later, the analysis results will be evaluated after the verification of the problem.

CHAPTER TWO

MODELLING OF DOUBLE PIPE CONDENSER

2.1 Problem Definition

For the numerical solution of a double pipe heat exchanger with the multi-phase flow, a one-dimensional mathematical model is developed. The developed model is used for both steady and transient solutions. Governing equations are solved in both steady-state and transient condition and consider the effects of phase transition on heat transfer and fluid characteristics.

In the double-pipe condenser, water as heat transfer fluid (HTF) is flowing inside the annulus of the condenser, and the refrigerant is condensing inside the inner tube, and heat transfer occurs as the refrigerant moves forward through condensation from the subcooled region and reaches the superheated state finally. A simplified schematic of the condenser model can be seen in Figure 2.1. In Figure 2.1, r_{in} and r_{out} represent the inner tube and outer tube radii, respectively. Geometrical properties and the flow characteristics will be given with the results according to the applied case.

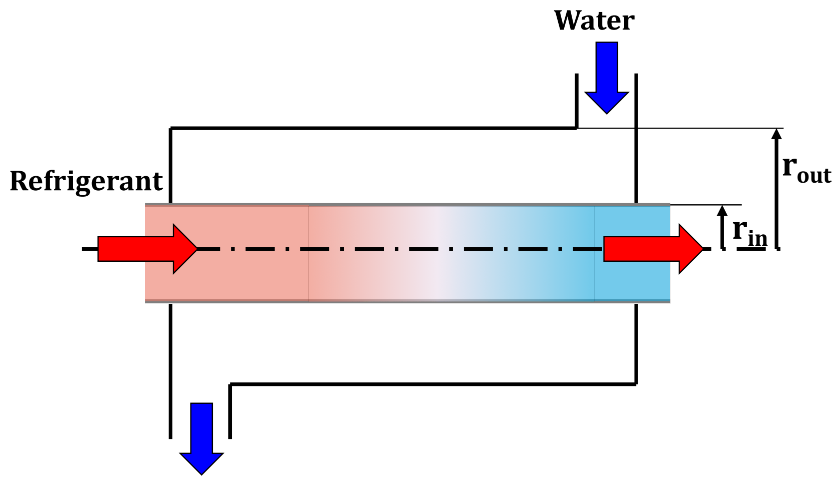

Figure 2.1 Schematic illustration of the developed condenser model

Refrigerant is chosen according to the most common applications in heat pump cycles. In this study, two frequently used refrigerants are chosen; R134a and

R1234yf. The purpose of solving this problem with different refrigerants is to see if alternative refrigerants that are thought to be less harmful to the environment can replace the old ones. Detailed results and comparisons will be explained in the following sections.

2.2 Mathematical Formulation

The mathematical model of the double pipe condenser is developed to reflect the effects of phase change. Even though both the single-phase and double phase flow requires knowledge about the heat transfer coefficient, which leads to the convection between two fluids, condensing flow is more complicated because of the changing flow characteristics. For this reason, first condensing flow will be explained in detail and after, equations used for condensing flow will be given.

In order to offer a general and holistic solution, equations are written in enthalpy form, which does not change depending on single or multi-phase. The developed model takes account of the condensing flow effects on the convective heat transfer and thermophysical properties of the refrigerant in every point inside the geometry.

For the model, the following boundary conditions are applied for the solution of the condensing flow;

- Flow is one dimensional along axial direction for both the refrigerant and HTF flow,
- Conductance inside the fluid and the tube walls are neglected,
- Convection is accepted the dominant heat transfer and radiation effects between surfaces are also neglected,
- Equations are solved for Newtonian fluid in steady and transient forms.
- For the energy definition, both the potential and kinetical effects are negligible.

Equations according to these assumptions have the following form;

Continuity:

$$\frac{\partial}{\partial t}(\rho)+\frac{\partial}{\partial z}(\rho u)=0 \tag{2.1}$$

Momentum:

$$\frac{\partial}{\partial t}(\rho u)+\frac{\partial}{\partial z}(\rho uu)=-\frac{\partial p}{\partial z}+\frac{\partial}{\partial z}\left[\frac{\partial}{\partial z}(\mu u)\right] \tag{2.2}$$

Energy:

$$\frac{\partial(uH)}{\partial z}=\frac{\partial H}{\partial t}+S \tag{2.3}$$

The term S is source term used for energy transfer. The energy equation can also be defined in more specifically as below,

$$\dot{m}_{in}h_{in}-\dot{m}_{out}h_{out}\pm q''A=\frac{d(mh)}{dt} \tag{2.4}$$

In momentum formulation, pressure change calculation requires information about the shear stress term, which is evaluated by means of two-phase friction coefficient, f_{tp}. Similarly, in the energy equation, the heat flux term is defined as $q'' = U_{TP}\ (T_{fluid} - T_{wall})$ convective heat transfer coefficient U_{TP}, together with the knowledge of the flow structure, that is, the volume occupied by the liquid and vapor phases.

Fluid flow inside the tube is divided into three sub-regions according to the vapor quality, which is defined as the ratio of vapor to the total refrigerant amount and can be evaluated by enthalpy values. Refrigerant enters the inner tube as superheated vapor, and when the saturation condition is achieved, vapor refrigerant begins condensing as it slowly becomes liquid. Finally, it exists as a subcooled or compressed liquid. The transition between these regions are defined according to the following ranges:

- Liquid region: $0 \leq x \leq 0.05$
- Two-phase region: $0.05 < x < 0.99$
- Vapor region: $0.99 \leq x \leq 1$

Due to the nonlinearity of the multi-phase model, buffer regions are defined close to the liquid region and vapor region. Calculations, especially in the two-phase region, need to be relaxed by applying these limits for the smooth transitions and avoid sudden thermophysical changes.

2.3 Condensing Flow

According to Wallis (1982), two-phase flow is an "*insecure*" science. This phenomenon is influenced by so many factors that limit the theoretic value unless it is supported by experiments. For the condensing flow, refrigerant does not simply transform into another physical condition but also its flow and thermodynamic behavior does change. The most common methods for solving multi-phase flows like condensing flow are empirical correlations, homogenous flow, and separate flow approaches. Using correlations for the prediction of two-phase behavior by calculating heat transfer and the friction coefficient is the "*simplest cookbook form of analysis*," as defined by Wallis (1982).

The governing equations used for the solution require the information of friction and heat transfer coefficient, which will be evaluated using empirical correlations. However, condensing and single-phase flow must be treated separately. Even though the mean considering properties for the fluid flow makes the solution process simpler, some of the local effects of phase transition would be lost due to the assumption of constant values. Instead of assuming mean, constant thermophysical conditions, this study is aimed to express heat transfer and friction term more detailed depending on the flow characteristics.

Condensing flow takes different shapes according to the orientation of the channel in which fluid flows. For example, in a vertically oriented tube, as the vapor began to liquefy, an annular condensate film forms on the surface of the tube. Alternately, vapor, and liquid distributions in a horizontal tube would be more complicated due to the perpendicular gravity force (Kandlikar (Ed.), 1999).

For the condensation in horizontal tubes, several different flow conditions can be seen as in Figure 2.2, which are given in the literature (W.M. Rohsenow (Ed.), Hartnett (Ed.), and Cho (Ed.), 1998). In this figure, saturated vapor enters the tube, and vapor quality, x is 1. As the vapor flows inside the tube, it begins condensing, and finally, after fully condensed, it leaves the pipe as the saturated liquid of which vapor quality, x equals 0. During the flow and phase transition, at first, fluid is mostly vapor, and the velocity of the vapor is high. Thus, high-velocity vapor channels the liquid part to the outside of the pipe, and this leads to the flow become annular. In other words, vapor shear stress is larger when compared to the gravity effect, and the liquid part is still small; thus, flow form becomes annular. In the annular flow zone, pressure and viscosity forces are in equilibrium (Stephan, 1992). In the next period, vapor velocity decreases as the vapor condenses, and the annular liquid film begins to take a bigger part of the pipe cross-section. In consequence of the lower vapor velocity, condensate flows through downwards with the influence of gravity. Vapor stays at the upper part, and growing liquid flows down to the bottom. Condensate film becomes very thin on the upper part at this stage, which leads to the heat flux variation and affects the energy transfer. At this stage, flow is called stratified. As the condensation continues, the vapor state becomes smaller and smaller until small bubbles, and finally, complete condensation will be achieved.

Calculation of friction and heat transfer coefficient can be made by using related correlation from the literature. The pressure gradient is commonly expressed by wall shear stress as a function of frictional effects in the fluid flow. The friction coefficient is calculated by using Churchill’s friction coefficient correlation (Churchill, 1977).

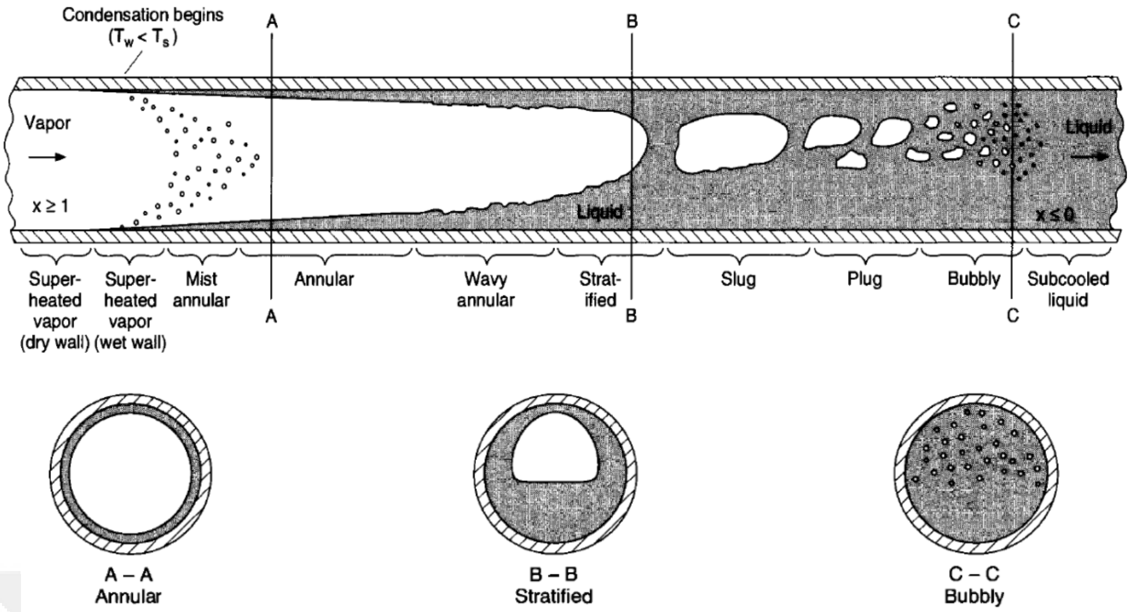

Figure 2.2 Condensing flow in a horizontal tube (Rohsenow (Ed.) et al., 1998).

Moreover, heat transfer is formed by convection between two phases. For the high mass flux, G values, the gravity effect can be neglected because if the mass flux is bigger than a certain value (can be taken as 400 kg/m^2s), heat transfer is dominated by forced convection (Kandlikar (Ed.), 1999). Different correlations are stated in the literature for the condensation with high mass fluxes. Cavallini's (Cavallini et al., 2001) and Shah's correlation (Shah, 1979) is one of the most commonly used in the industry. In addition, Dobson & Chato (1998), Fujii (1995), Bivens & Yokozeki (1994), Tandon, Varma, & Gupta (1995), and Tang, Ohadi, & Johnson (2000) also developed a correlation for the condensing flow in case of different operating conditions and different refrigerants.

In this study, Shah's condensation correlation will be used, and the determination process and the comparison of different equations will be explained in the verification section in detail (Section 2.5). Shah developed a simple-to-use correlation based on 474 experimental data from different refrigerants such as water, R11, R12, R13, methanol, ethanol, benzene, toluene, and trichloroethylene. He studied different types of orientation as horizontal, vertical, inclined, and also change the diameters between 7 mm and 40 mm. The equation is basically a modified Dittus-Boelter correlation (Shah, 1979).

Heat transfer and phase distribution are strongly dependent on the flow pattern. For the condensing flow when using Shah's correlation, two types of fluid flow are taken as the main flow patterns; annular and stratified flow. Shah's correlation is applicable for the below conditions based on his recommendation,

- Reduced pressure range: $0.002 \leq p_{red} \leq 0.44$ (kPa)
- Saturation temperature range: $22 \leq T_{sat} \leq 310$ (ºC)
- Vapor velocity range: $3 \leq u_g \leq 300$ (m/s)
- Vapor quality range: $0 \leq x \leq 1$ (-)
- Mass flux range: $10.8 \leq G \leq 1599$ (kg/m^{2}s)
- Liquid Reynolds number: $Re_l > 350$ for the tube
  $Re_l > 3000$ for the annulus.
- Liquid Prandtl: $Pr_l > 0.5$
- No limitation for the heat flux: q'' (W/m^2).

Refrigerant properties and operating conditions are appropriate by means of the correlation limits and will be given in detail in the later sections.

2.4 Numerical Solution

One dimensional model of the double pipe condenser, as shown previously in Figure 2.1, is divided into a number of specified control volumes. The spatial discretization of the condenser model can be seen in Figure 2.3.

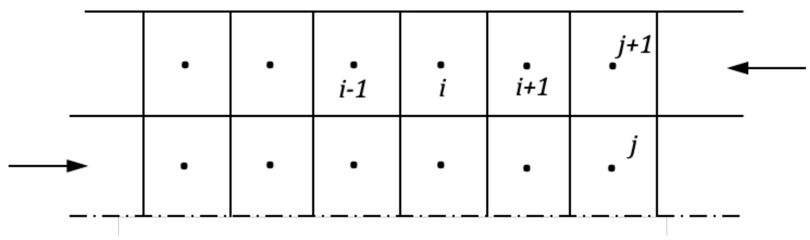

Figure 2.3 Spatially discretized condenser model

In Figure 2.3, *i, j* show the related control volume to be solved at a certain iteration. Governing equations are discretized using an explicit method, and the first-order Upwind scheme in the flow direction is used. The general illustration of the Upwind scheme application on the control volume can be seen in Figure 2.4.

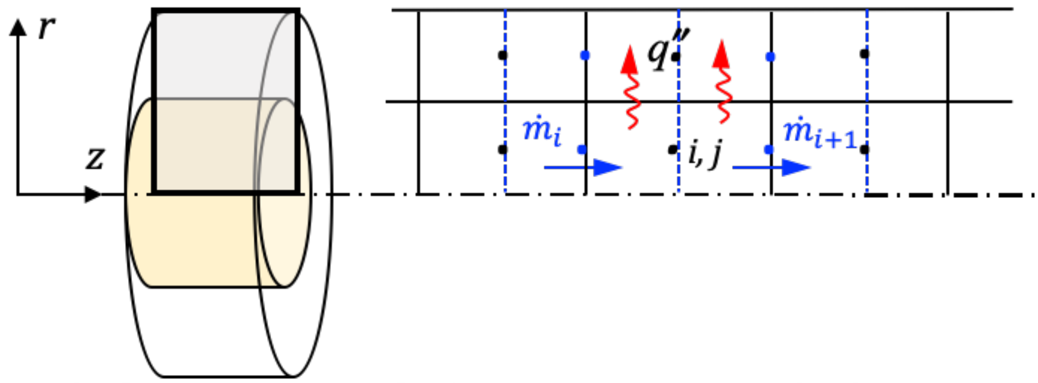

Figure 2.4 Upwind scheme applied control volume

Transient terms of the governing equations are discretized using the three-time level approximation (Dupont, 1974),

$$\frac{\partial \phi}{\partial t} = \frac{3\phi - 4\phi^{0} + \phi^{00}}{2\Delta t} \tag{2.5}$$

In Equation 2.5, Δt is the time step size, and ϕ refers to a general dependent parameter. When it has one and two zeros as superscript, this means the value of the previous and the second previous time step, respectively. This scheme, differently from the two-time level scheme, provides advantages such as smaller truncation error and greater stability (Ozisik, 1994).

The discretized momentum equation is solved for the pressure distribution along the pipe, and the energy conservation is obtained by the rate of enthalpy change in the refrigerant, which equals heat transfer at the boundary between inner pipe and annulus. Transient terms in continuity and momentum equation are not solved and assumed as negligible. Finalized governing equations are discretized as below in both spatial and temporal manner;

Continuity:

$$\dot{m}_i = \dot{m}_{i+1} \tag{2.6}$$

Momentum:

$$(p_{i+1} - p_i)A_c = \tau P \Delta z \tag{2.7}$$

Energy:

$$\dot{m}_i h_i - \dot{m}_{i+1} h_{i+1} \pm q'' A = \frac{m(3h - 4h^0 + h^{00})}{\Delta t}$$

$$q'' = h_{conv}(T_{i,j} - T_{i,j+1}) \tag{2.8}$$

2.4.1 Calculation of Empirical Coefficients

In the momentum equation, τ as shear stress on the tube wall is calculated as a function of friction coefficient, and the formula can be seen from Equation 2.9, and the friction coefficient is taken as Fanning friction factor. Pressure drop along the pipe is calculated by taking frictional effects account using Churchill's equation (Churchill, 1977), which is given in Equation (2.10). This equation can be applied for both single-phase and two-phase flow.

Wall shear stress:

$$\tau = f \frac{\rho u^2}{2} \tag{2.9}$$

Churchill's friction coefficient equation (Churchill, 1977):

$$f = \left[\left(\frac{8}{\mathrm{Re}} \right)^{12} + \frac{1}{(A+B)^{3/2}} \right]^{1/12}$$

$$A = \left[2.457 \ln \frac{1}{\left(\frac{7}{\mathrm{Re}} \right)^{0.9} + \frac{0.27\varepsilon^*}{D}} \right]^{16} \tag{2.10}$$

$$B = \left(\frac{37530}{\mathrm{Re}} \right)^{16}$$

In this equation, A and B is the specifically developed coefficients empirically and $\frac{\varepsilon^*}{D}$ is the ratio of tube material roughness to the diameter or so-called relative roughness which is taken 0 due to its negligible effect in this study. Re referred to flow Reynolds number and defined as Re $= \rho VD/\mu$ or Re $= GD/\mu$. However, if the flow becomes multi-phase, then special calculation must be made in order to obtain the two-phase Reynolds number, which is a function of two-phase viscosity.

Two-phase Reynolds Number:

$$\mathrm{Re}_{TP} = \frac{GD}{\mu_{TP}}$$

$$\mu_{TP} = x\mu_g + (1-x)\mu_l \tag{2.11}$$

Secondly, the convection term in the energy equation is the function of the heat transfer coefficient, which will be obtained using different equations according to the flow condition. For the single-phase condition in the inner tube and the annulus, the Gnielinski equation (Gnielinski,1983) is used. This equation has been using for the turbulent flow, and the heat transfer coefficient is calculated as a function of Nusselt number, Nu $= h_{conv}D/k$. The only difference for the annulus flow is the diameter term, *D,* which will become hydraulic diameter, D_h, in case of the annulus.

*Gnielinski's correlation for single-phase, turbulent flow (*Gnielinski, 1983)*:*

$$Nu = \frac{(f/8)(\mathrm{Re}-1000)Pr}{1+12.7\sqrt{f/8}(Pr^{2/3}-1)}\left[1+\left(\frac{D}{L}\right)^{2/3}\right]$$

$$f = (1.82\log_{10}\mathrm{Re}-1.64)^{-2} \tag{2.12}$$

For the two-phase flow inside the tube during condensation, Shah's correlation is used, as mentioned in the previous sections. This correlation offers a broad application ability, even if there are different refrigerant types or geometric conditions.

Shah's correlation for heat transfer coefficient in condensing flow (Shah, 1979):

$$Nu = 0.023(\mathrm{Re}_l^{0.8})(Pr_l^{0.4})\left(1+\frac{3.8}{p_{\mathrm{red}}^{0.38}}\right)\left(\frac{x}{1-x}\right)^{0.76} \tag{2.13}$$

In this equation, Reynolds and Prandtl numbers are liquid Reynolds and liquid Prandtl numbers, they are calculated using the liquid phase properties, and p_{red} is the reduced temperature, which is the ratio of fluid pressure to the critical pressure:

Liquid Reynolds number:

$$\mathrm{Re}_l = \frac{GD(1-x)}{\mu_l} \tag{2.14}$$

Liquid Prandtl Number:

$$Pr_l = \frac{\mu_l c_{p,l}}{k_l} \tag{2.15}$$

Reduced Pressure:

$$p_{red} = \frac{p}{p_{critical}} \tag{2.16}$$

2.4.2 Solution Algorithm

The solution process is carried out at each time step by solving the main algorithm. At each time step, calculations of discretized equations are made until the convergence is achieved. At the beginning of the solution, the inlet boundary condition is applied to the inner pipe and annulus. In each iteration, guessed values from the previous iteration and the calculated ones are compared. From the known and guessed values at the inlet, variables are calculated at the outlet of the control volume from the discretized equations iteratively. At that current iteration cycle, calculated values at the outlet become the inlet values of the next control volume, and this goes on until the end of the condenser tubes. If the phase change between vapor and liquid state takes place, then the point of transition is assigned to the outlet of the control volume. At each control volume, convergence is controlled by a defined criterion, ε, and the convergence condition can be shown as follows;

$$\frac{\left|\phi^* - \phi\right|}{\bar{\phi}} \le \varepsilon \tag{2.17}$$

In this equation, ϕ^* is the value of a parameter from the previous iteration. The error is calculated between two iterations by taking the absolute value of the maximum difference between two parameters and is divided by the mean value of that parameter. This value should be smaller or equal to the defined convergence criteria. In this study, this criterion is defined as 10^{-6} for the condenser model. Error is calculated temperature, and the enthalpy and the solution cycle does not proceed to the next time step until the convergence is achieved for both of these parameters.

Thermophysical properties of the refrigerant and heat transfer fluid are evaluated using enthalpy, temperature, pressure, or vapor quality from the REFPROP NIST Database (REFPROP v.6.01. NIST) depending on the state of the fluid.

For the solution of the developed numerical algorithm, MATLAB software is used. Governing equations with the inlet conditions and guesses as input values are solved as previously described step-by-step. The flow chart of the algorithm can be followed in Figure 2.5.

From the initial to the last time step first heat transfer coefficient is calculated with the obtained fluid properties, and then pressure loss is evaluated. For the numerical solution explicit scheme is used, moving forward step by step in the flow direction. The coefficient matrix of enthalpy and temperature is solved using TDMA (Tri Diagonal Matrix Algorithm). Finally, according to the enthalpy distribution, vapor quality is calculated, and the temperature value in each control volume is updated accordingly.

Results are obtained in both steady-state and transient situations. In both cases, energy conservation is considered as the main reliability criterion. After the solution is made, energy balance is basically a comparison between the rejected heat from the condensing refrigerant by means of enthalpy, and the gained heat by the water by means of temperature is checked.

In order to provide a reliable solution, solution characteristics such as time-step and mesh number must be appropriately chosen; otherwise, it will inevitably affect the quality of the solution. A preliminary parametric study is conducted to ensure the selected time-step and grid size. Different grid sizes are applied for the same problem, and grid-independency analyses are made.

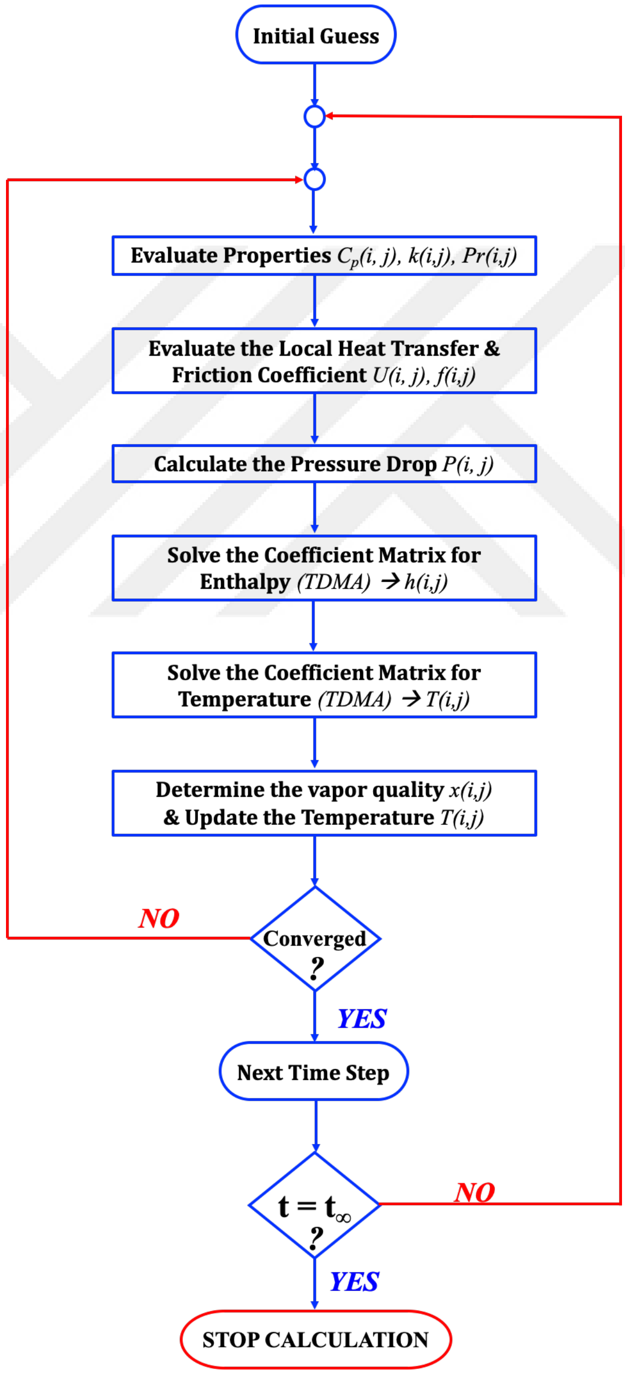

Figure 2.5 Solution algorithm for condenser model

After deciding on the mesh number, the problem is solved for different time-step values, similarly. Different parameters selected for the mesh number and time-step and the related results can be seen from Table 2.1 and Table 2.2, respectively. In both mesh number and time-step-independency tables, *% Error* refers to the energy conservation between refrigerant and heat transfer fluid.

Table 2.1 Mesh number independency

Mesh Number	***Inner Pipe Outlet Temperature, ºC***	***Annulus Outlet Temperature, ºC***	***% Error***
50	30.619	26.087	0.36
100	30.596	26.067	0.16
150	30.296	26.089	0.13
200	30.343	26.081	0.09
250	30.231	26.089	0.08
300	30.351	26.077	0.06

For the mesh number analysis, the coarsest and finest case is formed with 50 and 300 mesh number, respectively. Although the outlet temperatures of the inner tube and annulus are not stable enough to relate, energy conservation values, % Error was used to interpret the values. Error is 0.36% at the coarsest mesh number and 0.06% at the finest. In this study, the error value below 1% was accepted as an indicator that the problem was solved with sufficient accuracy. The selected grid size as 150 differs from the finest, only 0.06% from the finest with a 0.12% error, which is acceptable. Table 2.1 shows that even though grid size with 300 meshes provides a reasonable accuracy, it will take longer to complete the whole solution since increasing the number of mesh take a longer time to convergence. Thus, 150 is taken as the grid size, and this option offers quite a good accuracy and less computation time.

Secondly, for time-step-independency analysis, the smallest and biggest time-steps are taken as 0.01 s and 0.5 s, respectively. If the outlet temperature values are examined, it is clearly seen that the temperature has remained constant for all selected time steps except the largest time step. The *% Error* value shows a similar trend. For this reason, an evaluation other than the greatest error value was made, and as a result, an average time step of 0.1 s was chosen, which would both provide reliable results and not extend the solution-time.

Table 2.2 Time-step independency

Δt, s	***Inner Pipe Outlet Temperature, ºC***	***Annulus Outlet Temperature, ºC***	***% Error***
0.01	30.296	26.089	0.127
0.05	30.296	26.089	0.127
0.10	30.296	26.089	0.127
0.25	30.2966	26.089	0.127
0.50	30.343	26.081	0.095

For both of the mesh number and time-step analysis, results for the variation of heat transfer coefficient value with time also analyzed and can be seen in detail from Figures 2.6 and 2.7.

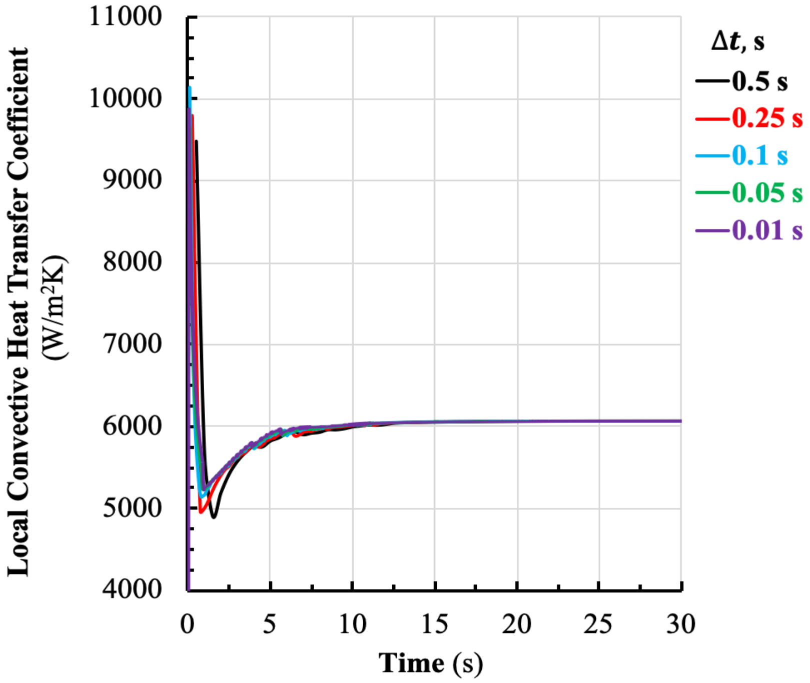

Figure 2.6 Variation of heat transfer coefficient for different time-steps

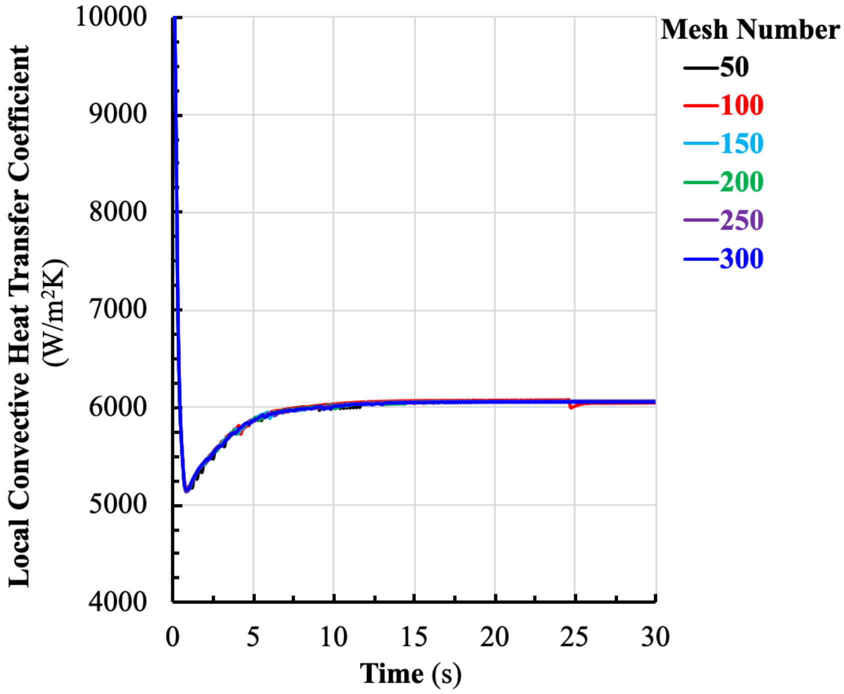

Figure 2.7 Variation of heat transfer coefficient for different mesh numbers

Similarly striking in both charts is that large changes occur in the first steps of total time. In fact, it is seen that the different time steps and mesh numbers used after a while will not have significant effects on solving the problem. From the time-wise comparative figures, it was found that the time-step size of 0.1 s, and the mesh number of 150 are optimum for accuracy and computational time.

2.5 Verification

The developed algorithm is used to solve a multi-phase flow problem within a shell-and-tube type geometry. The verification of this algorithm is crucial in order to ensure that results are reliable for making conclusions.

For verification of the solved condenser model, experimental data and different empirical equations from the literature are used. García-Valladares (2003) made comparisons for different conditions using experimental data from the literature. They have applied the most commonly used empirical equations to the relative experimental case and analyze the differences between them.

Experimental results from Shao and Granryd (2000) and the results of García-Valladares (2003) are used to investigate the differences between their results and developed algorithm when the same correlations are applied. García-Valladares (2003) made a comparison between the experimental data by Shao and Granryd (2000) and most preferred empirical equations from Shah (1979), Dobson and Chato (1998), Cavallini et al. (2001), Fujii (1995), Bivens and Yokozeki (1994), Tandon et al. (1995) and Tang et al. (2000). In the case of the experiment, refrigerant R-134a flows through a 6 mm inner diameter tube with G = 183 kg/m^{2}s mass flux and a saturation temperature of 30ºC. In their study, wall temperature is not given. Thus, wall temperature is assumed to be between 20ºC and 25ºC. Shao and Granryd (2000), stated uncertainty in the heat transfer coefficient between 10% to 15%; for this reason, an error bar of 15% has been applied to Figures 2.8 and 2.9.

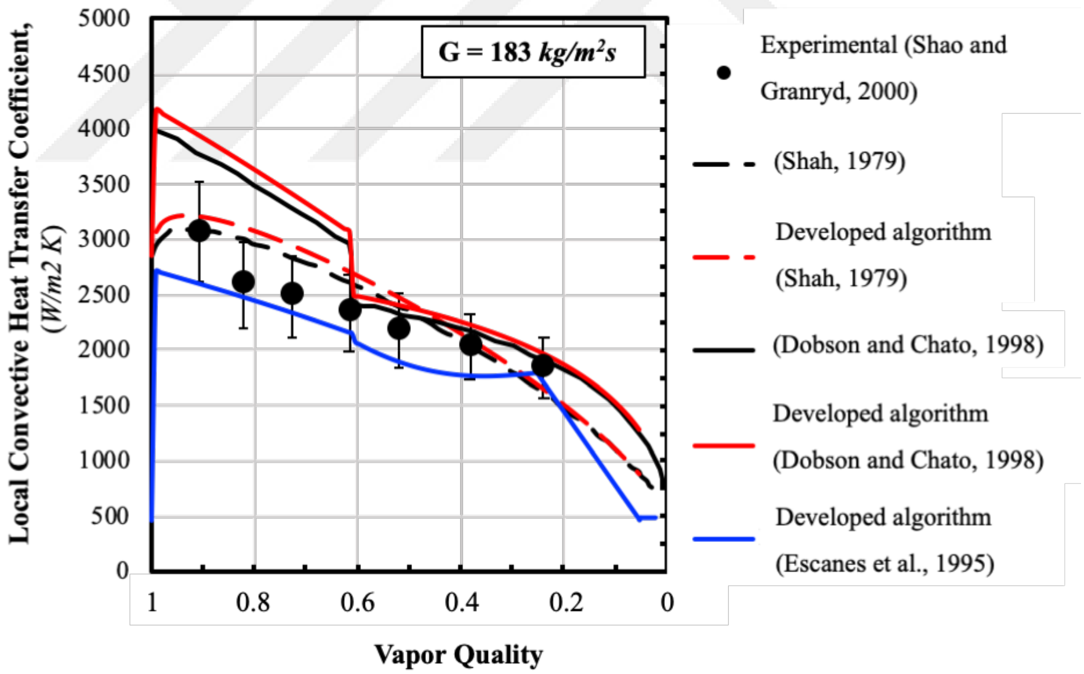

Figure 2.8 Comparison of correlations with the current numerical algorithm (Shao & Granryd, 2000; Shah, 1979; Dobson & Chato, 1998; Escanes et. al., 1995)

Even though there were more different correlation results in García-Valladares (2003), two commonly used equations are chosen to evaluate the case, Dobson and Chato (1998) and Shah (1979).

In addition, equations applied in Escanes et al. (1995) are also analyzed in the developed algorithm due to the similarity of the problem, which is solved in Escanes et al. (1995). According to the study by Escanes et al. (1995), the heat transfer coefficient is calculated using Jaster and Kosky (1976) for stratified flow. For annular flow, the expression was proposed by Boyko and Kruzhilin (1969). As a transition criterion between different flow patterns, the equation of Wallis (1969) is used.

In Figure 2.8, the aim was to examine whether the algorithm runs appropriately when the same correlations are applied within the study of García-Valladares (2003). Results depicted that the solution algorithm provides consistent results with García-Valladares (2003) study. Both of the black-dashed and smooth-lines show fairly close behavior when compared to the results from García-Valladares (2003), which can be seen from the red lines. It has been thought that the reason for the small gap between lines can be caused by using different pressure loss calculations by different friction coefficients.

In addition to the previous figure, one additional analysis with a higher mass flux value is made. The purpose of trying different flow conditions is to determine the most suitable one for the selected problem in this study. For the second analysis, there is no comparison between the García-Valladares (2003) results and the algorithm. However, the same correlations from the previous validation analysis are used to compare empirical equations themselves.

For this analysis, experimental data from Cavallini et al. (2001) is used. Cavallini et al. (2001) carried out the experiments for condensation of again R134a and inside an 8 mm diameter tube with mass flux ranging from 200 to 750 kg/m^2s. The saturation temperature is 40ºC, and the vapor quality varies between 0.2 and 0.8. Numerical results for correlations are taken from the developed algorithm. The results are given in Figure 2.9.

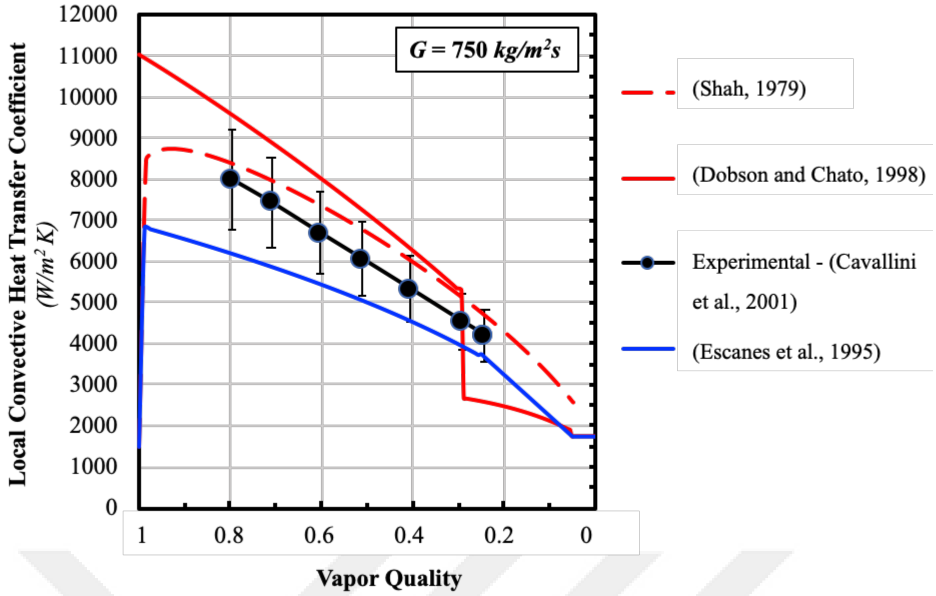

Figure 2.9 Comparison of correlations for R134a during condensation (Shah, 1979; Dobson & Chato, 1998; Cavallini et. al, 2001; Escanes et. Al., 1995)

According to the comparison between empirical correlations and experimental data presented in both Figures 2.8 and 2.9, the equation by Shah (1979) is appeared to be the most accurate, and it shows more similar behavior with the experimental data in lower and higher mass flux value comparing to Dobson and Chato (1998) and Escanes et al. (1995).

In conclusion, after comparing different correlations presented in the literature, for the annular and stratified type of condensation Shah's correlation, *i.e.*, Equation 2.13, is found to be the most appropriate one.

2.6 Results for Double Pipe Condenser

Results are obtained for the double pipe condenser with water as heat transfer fluid. Two different refrigerants are used for the condensing flow; R134a and R1234yf. R1234yf is a new alternative used to replace R134a due to adverse environmental effects. In order to analyze the flow inside the condenser, a number of evaluations are made by varying different parameters such as mass flux, pipe diameter ratio between inner and outer pipe, refrigerant. While investigating the specified effect for the flow, all the remaining parameters are held constant. For all the results, the saturation temperature is set to 45ºC. For the analysis other than those in which diameter ratio is analyzed, inner and outer diameter equals 6 mm and 16 mm, respectively.

2.6.1 Effect of Mass Flux

In Figure 2.10, the variation of the heat transfer coefficient for the R134a is given in different mass fluxes. Values are obtained locally and in a steady-state condition. Four different mass fluxes are compared; 200 kg/m^{2}s, 400 kg/m^{2}s, 600 kg/m^{2}s and 884 kg/m^{2}s. Reynolds numbers for these mass flux values are also calculated accordingly and can be seen in the figure. The mass flow rate of the water flowing in the outer tube is 0.1 kg/s in this case.

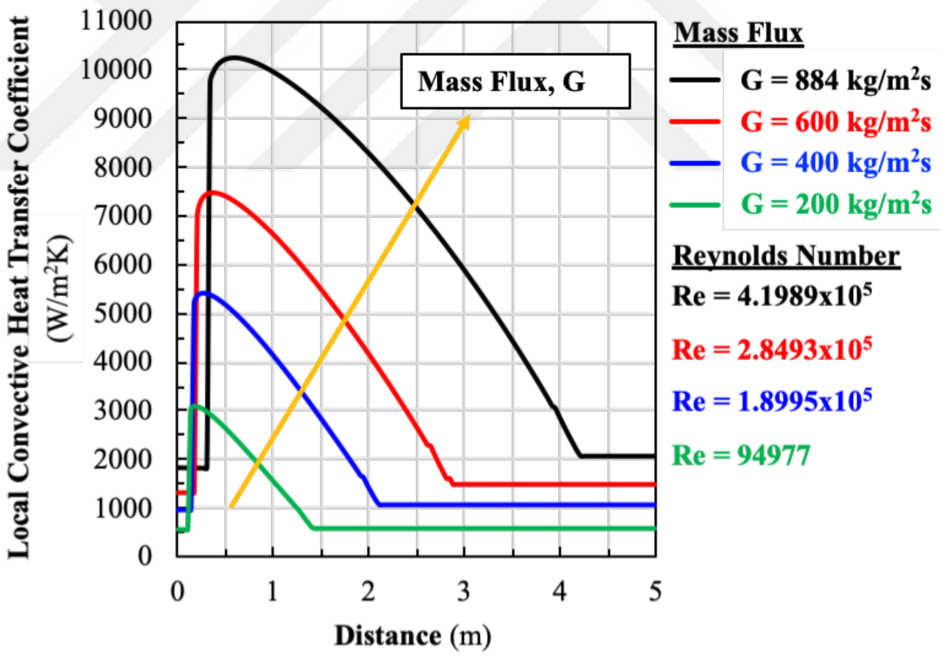

Figure 2.10 Variation of heat transfer coefficient in steady-state

In Figure 2.10, it can be seen that increasing mass flux gives a higher heat transfer coefficient, which is due to the mass flow rate of the refrigerant becomes bigger for the same surface area. The effect can be realized, especially in the two-phase region, which can be understood by the peaks on each curve. For the minimum value of mass flux, the heat transfer coefficient is roughly 950 W/m^{2}K, and in the maximum case, its average value is approximately 6000 W/m^{2}K. The increase in the heat transfer coefficient is predictable since it highly depends on the Reynolds number. Higher mass flux values also make the condensing flow region larger. In the case of a single-phase, the value of the heat transfer coefficient is constant. While the range where the curve does not remain constant and varies between 0.2 m and 1.4 m at the smallest mass flux, the same change is between 0.4 m and 4.2 m at the highest mass flux.

Similarly, the effect of varying mass flux values is also investigated in a transient state, and results are given in Figure 2.11 for only a short period of time since the value becomes stable and constant after approximately 15 seconds. Similar effects to the previous simulation are observed; higher mass fluxes lead higher values of heat transfer coefficient.

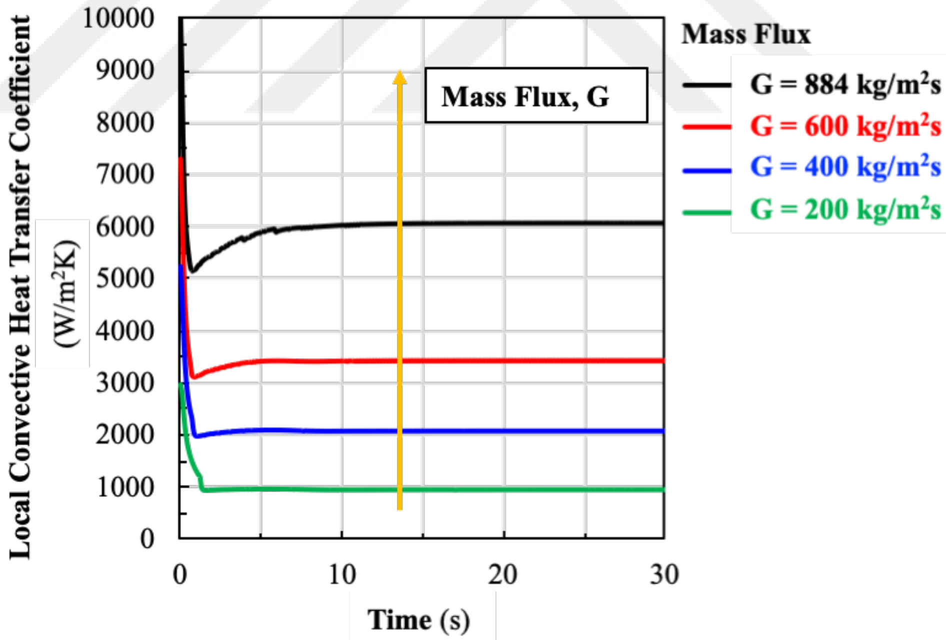

Figure 2.11 Variation of heat transfer coefficient in transient condition

The results showing the effects of varying mass fluxes and diameter ratios on the pressure distribution along the tube for the refrigerant side are presented in Figure

2.12. The mass flow rate of the HTF is the same as previous simulations, and the refrigerant is R134a.

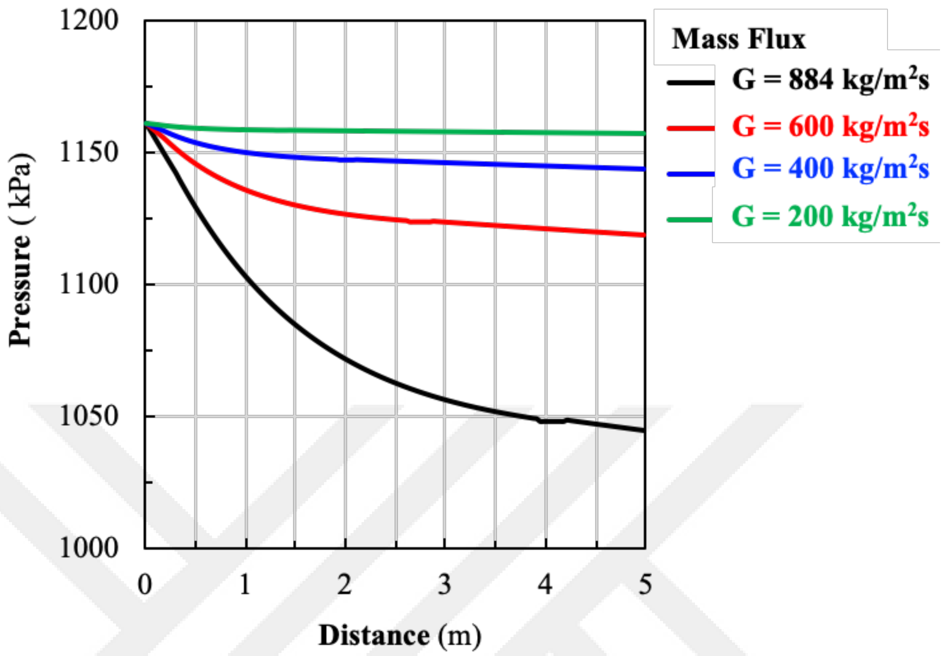

Figure 2.12 Variation of pressure by the mass flux

From Figure 2.12, it is found that the higher the mass flux value gives, the greater the pressure change across the tube, proportionally. The pressure drop is roughly 95 kPa in the case of 884 kg/m^{2}s mass flux through the tube and nearly zero at the lowest mass flux. In cases with higher mass fluxes, there is a non-linear behavior of pressure with distance. The reason for that is the significant changes in density, which is no longer negligible. Changes in density are caused by velocity becomes significant at higher mass fluxes.

2.6.2 Effect of Diameter Ratio

The effect of the diameter ratio on the spatial temperature variation is investigated in Figure 2.13. The diameter ratio is calculated by varying the outer and inner diameter of the tubes, and five different values are analyzed as 1.5, 2, 2.67, 3, and 4. The case with a 2.67 diameter ratio is the standard condition that is used in the other simulations.

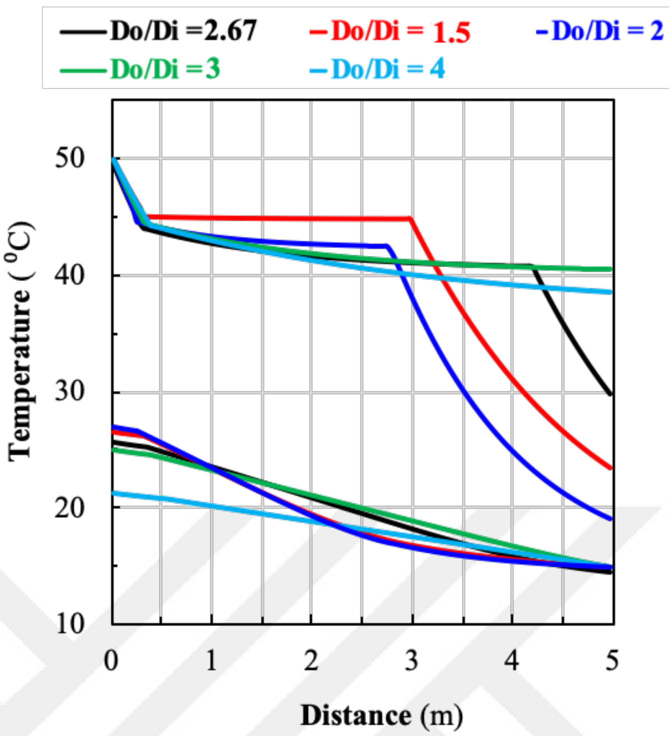

Figure 2.13 Variation of temperature by varying diameter ratios

Typically when the diameter ratio is 2.67, a phase change occurs between 0.15 m and 4.20 m. There is a slight pressure drop in both sides of the heat exchanger. On the other hand, when the diameter ratio goes higher or lower, it affects the phase change region and heat transfer, correspondingly. For the 5 m long tube, condensation does not complete when the diameter ratio equals or more significant than 3. In contrast, it becomes concluded in the shorter region when the diameter ratio is smaller than 2.67. However, there is not a straight-forward relationship because when the diameter ratio equals to 1.5, which is smaller than the case diameter ratio is 2, and the condensation still occurs for longer than the cases as mentioned above. A detailed table of the parameters investigated relating this simulation is given in Table 2.3. In this table, one can see the subcooling degree and the vapor quality for the cases in which condensation is not completed. Required condenser length according to the desired subcooling degree needs to be decided by taking account of the diameter ratio.

Table 2.3 Diameter ratios with subcooling and vapor quality at the outlet

D_{outer} (mm)	D_{inner} (mm)	D_{outer}/D_{inner}	*Subcooling* (°C)	*Vapor Quality*
15	10	1.5	21.3	0
12	6	2	23.4	0
16	6	2.67	11	0
18	6	3	-	0.002
24	6	4	-	0.39

The other parameter of which the effect of different diameter ratios is investigated is the heat transfer coefficient. The purpose of doing this simulation is because the heat transfer coefficient is directly linked to the energy transfer rate. The results are given in Figure 2.14.

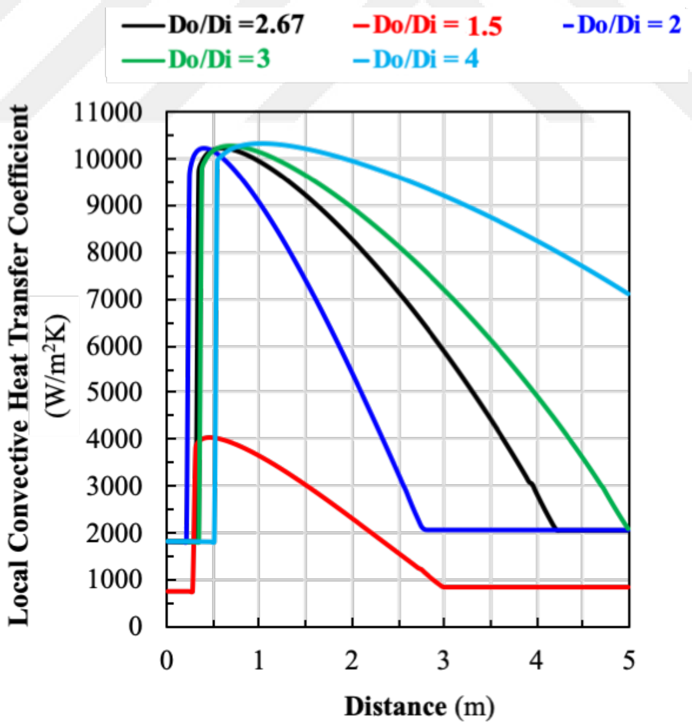

Figure 2.14 Variation of heat transfer coefficient by varying diameter ratios

From Figure 2.14, it is seen that the values of the heat transfer coefficient are lower than the other cases when the diameter ratio is 1.5. As it is previously mentioned, the phase changing process takes longer when the diameter ratio is bigger. This is the reason why the local heat transfer coefficient has bigger values because, in the two-phase region, the heat transfer coefficient is dramatically higher than both of the single-phase regions, vapor, and liquid. Nevertheless, after some point, the maximum value of the heat transfer coefficient is not influenced by the growth of the diameter ratio.

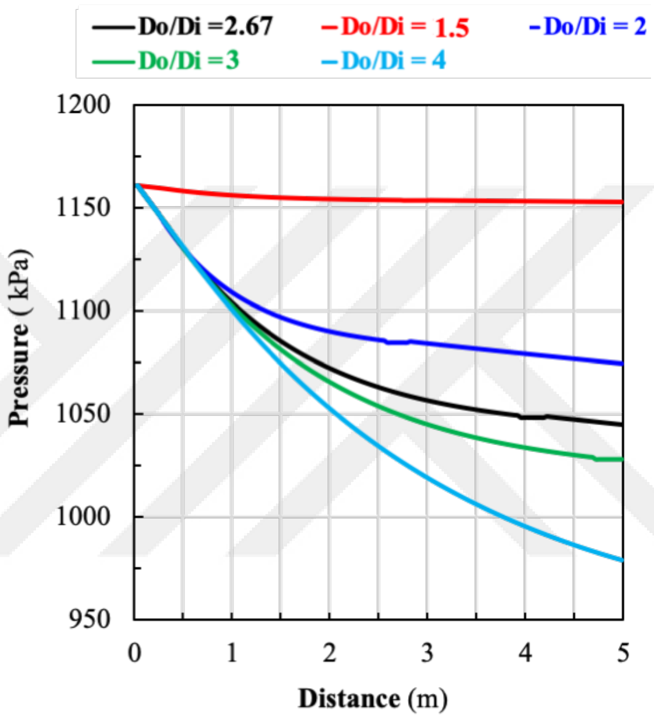

Figure 2.15 Variation of pressure by changing diameter ratios

In Figure 2.15, results showed that when the difference between inside and outside diameters gets bigger, the pressure drop occurs faster and with a higher value. In the standard condition which is used for this study of condensation, the aspect ratio is 2.67, and the pressure drop is approximately 95 kPa. In the case with aspect ratio equals 1.5, the pressure decreases around 10 kPa, and around 185 kPa for the case with an aspect ratio is 4.

In the conclusion of pressure simulations, it can be generalized that the decrease in pressure is higher at the beginning of the tube and slowly decreases in the axial direction. This is due to the liquid form takes place in the early zones of the tube, and it increases the frictional losses resulting from pressure loss. Moreover, as the condensation process continues, vapor quality reduces by the heat rejection of the refrigerant. As a consequence of that, both phase velocity becomes lower, which leads to the pressure loss. However, even though there are different effects of condensing flow causes pressure loss, the final result is actually a small decrease, which can be neglected when designing a condenser. Thus, the next section of modeling condenser with PCM will be analyzed without pressure loss effects.

Another parameter obtained to examine the condensate flow is the vapor quality, which equals 0 at the beginning because refrigerant enters the condenser tube as a subcooled liquid. Variation of vapor quality along the tube is given under the condition of changing diameter ratios in Figure 2.16.

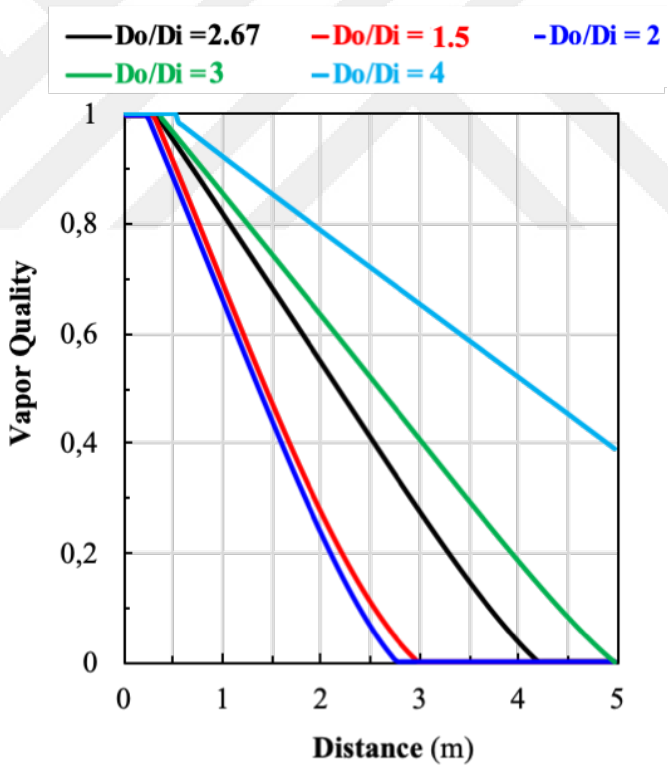

Figure 2.16 Variation of vapor quality by changing diameter ratios

The beginning and endpoint of the condensation process can be observed by vapor quality change. The vapor quality signifies the rate of vapor amount to the liquid amount. In the initial point of condenser, the refrigerant is in the superheated vapor state. After a while, as the water gives the fluid its heat, the refrigerant condenses. According to the results given in a related figure, when the dimeter ratio rise, phase change starts later, also it needs a longer distance to be fully completed.

2.6.3 Temperature Distribution

Furthermore, the temperature distribution is given in Figure 2.17 for the different instances in order to evaluate the variation of both HTF and refrigerant temperature with time.

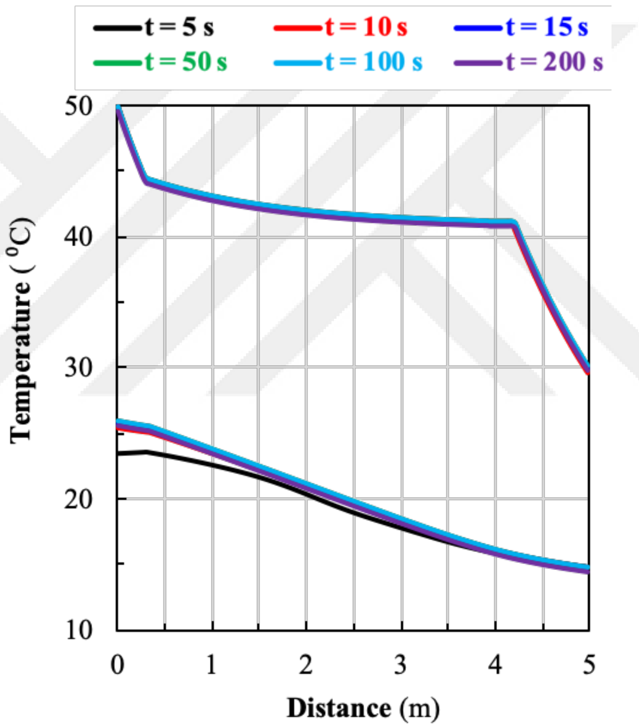

Figure 2.17 Variation of Temperature in different instances

In Figure 2.17, curves above and below the figure refer to the refrigerant and HTF temperature, respectively. When the flow becomes two-phase, temperature supposed to be constant in the ideal case. However, a slight temperature drop occurs due to the pressure drop along with the heat exchanger. In this case, refrigerant R134a with 0.025 kg/s mass flow rate flows through the condenser tube, and the water as heat transfer fluid with 0.1 kg/s mass flow rate passes from the annulus. As the R134a transfers its heat to the water, the condensation begins. From approximately 13 s from the initial state, the flow becomes steady as it can be realized the curves fit in a row after 10 s. There is a slight difference between the curves drawn towards the end of the period. The reason for that is the small variations of the thermophysical properties and the heat transfer coefficient due to the pressure drop. The phase changing process begins at 0.35 m and completely condensed at 4.2 m. Water is heated by around 10ºC. It enters the heat exchanger at 15ºC and exits 25ºC.

2.6.4 Effect of Refrigerant

R1234yf is analyzed as a better alternative to R134a, which has a bad impact on the environment. For the last decades, global warming potential value (GWP) became more important since it is found that refrigerants which are used in the industry, have a big part of the green gas emissions and global warming. To use more environmentally friendly refrigerants it has become a rule and determined by the international, global contracts (EU Regulation No 517/2014). R134a is a commonly used refrigerant. However, its GWP value is relatively high, and it will not be available after a certain time due to the regulations. R1234yf, on the other hand, has been seen as a strong alternative to the R134a and can be replaced the systems in which R134a were being used (Linde-gas, R1234yf – Opteon® YF brochure). In Table 2.4, a general comparison between R134a and R1234yf is given.

Table 2.4 Comparison of R134a and R1234yf (Prather, 2017)

Refrigerant	***Efficiency***	***Safety***	***Environment***	***ODP***	***GWP***
R134a	✓✓✓	✓✓✓	✓	0	1430
R1234yf	✓✓✓ *	✓✓	✓✓✓	0	4

*COP value of R1234yf is lower by 1.3-5% lower than R134a for the same cooling capacity (Daviran et al., 2017).

Beyond the comparison of environmental, safety, and efficient points, these two refrigerants also have similar saturation pressures and temperatures. Thus, in a refrigeration cycle, operating pressures and temperature would be highly similar when the refrigerant is replaced.

Results are obtained for both of the refrigerants in order to evaluate the thermal performance of the new alternative gas, and they can be seen from Figure 2.18 and 2.19.

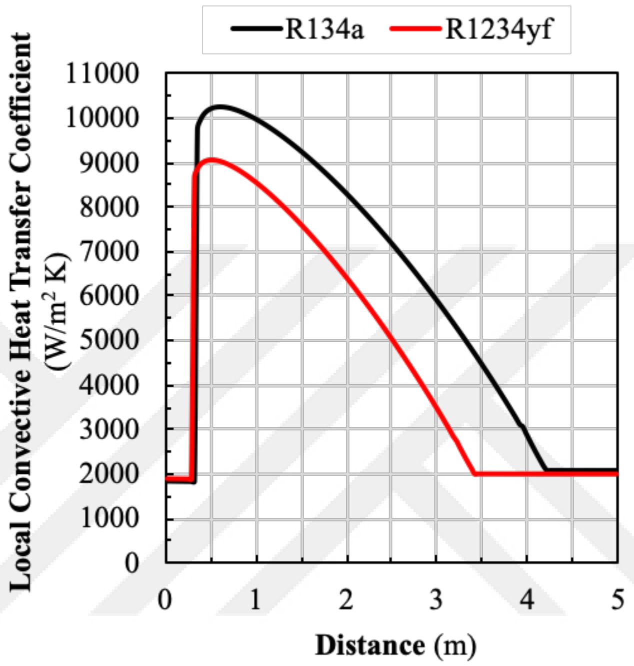

Figure 2.18 Heat transfer coefficient during condensation for R134a and R1234yf

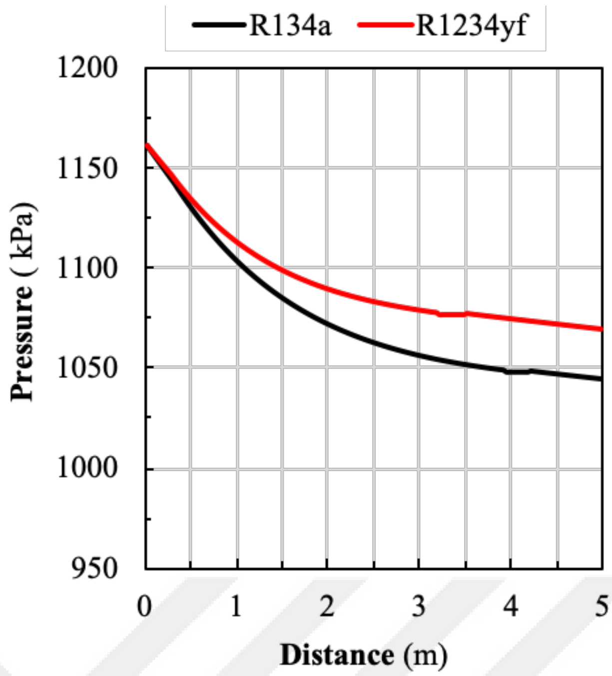

Figure 2.19 Pressure distribution during condensation for R134a and R1234yf

For Figure 2.18, the same operating temperature and pressure are used. Geometrical properties and the mass flow rates of both HTF and refrigerant were the same. In this condition, it can be seen that R134a provides a 22% higher heat transfer coefficient when the mean value through the condenser is obtained. Furthermore, in Figure 2.19, R1234yf gives a 2% higher pressure loss when compared in the exact same conditions. For both of the simulations, results were obtained in a steady-state condition.

In light of that information, temperature as another parameter is examined. For both of the refrigerants, refrigerant and HTF behaviors are given in different instances in Figure 2.20.

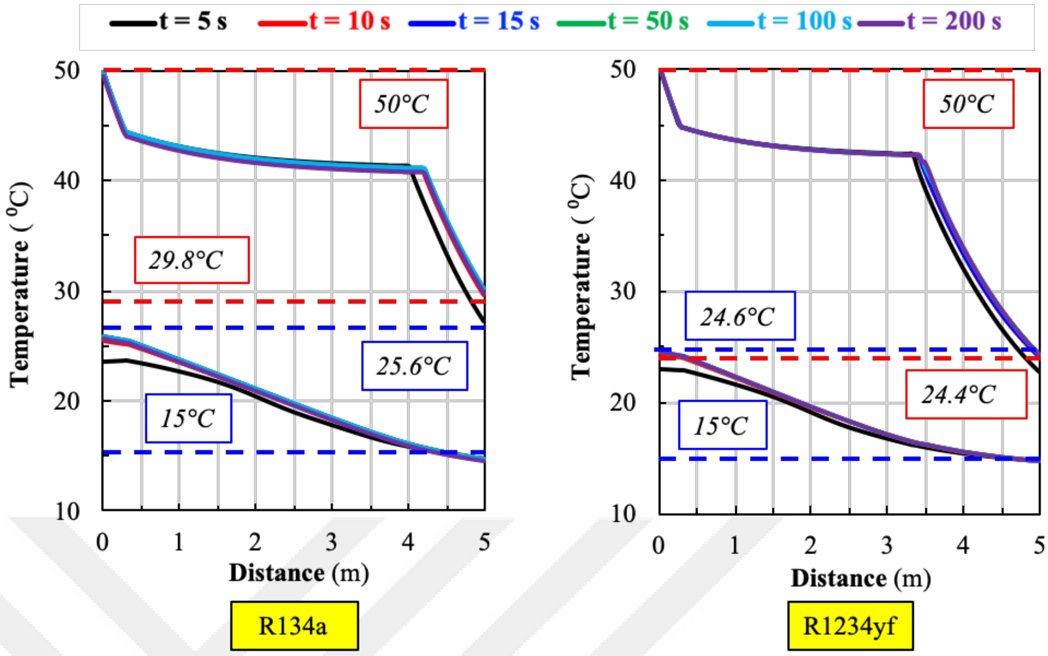

Figure 2.20 Temperature distribution inside the condenser for R134a and R1234yf

According to Figure 2.20, in the case of the same operating conditions, there are slight differences in outlet temperatures of refrigerant and HTF. For both of the refrigerants, the inlet temperature was set to 50ºC, and for the HTF, it was 15ºC. When the outlet refrigerant temperature is compared, it was 29.8ºC in the first case with R134a and 24.4ºC in the latter. On the other hand, for HTF, the outlet temperature of R134a was slightly higher as 1ºC than the outlet temperature of R1234yf. In general, R1234yf gives 12% higher heat transfer, and condensation completes for a shorter region of the condenser. Pipe length for a fully complete condensation becomes smaller.

CHAPTER THREE
MODELLING OF PCM CONDENSER

3.1 Problem Definition

The developed condenser model, which is explained in detail in previous sections, is used to analyze a condenser with PCM application around the inside tube. According to the problem in this thesis, the first PCM is in solid-state, and its temperature is slightly below the melting temperature. As the refrigerant begins flowing as superheated vapor, energy transaction from the refrigerant to the PCM takes place. While transferring heat, refrigerant reaches its saturation temperature will begin condensing. PCM, on the other hand, will start melting, and at some point, two kinds of multi-phase states will be present at the same time. Even though condensing flow is numerically solved in the previous part of this study, solidification and melting of the PCM would require special treatment for the solution procedure.

First, the numerical solution of heat transfer between phase changing PCM and the HTF with single-phase flow has been focused. The problem from Gong and Mujumdar's study (1997) is solved for the developed algorithm, and the problem is validated through the numerical results, which will be discussed in more detail in the next section. After verifying the scenario with HTF and PCM solution steps, condensing flow will be solved as a next step. PCM condenser is modeled with two kinds of fluid flow, the first refrigerant flows inside the tube, and then according to the outlet temperature, HTF begins flowing inside the outer tube, which is around the PCM layer. Refrigerant flow at the beginning is limited, depending on the outlet temperature. Normally, the condenser is modeled so that the refrigerant always comes out as a compressed liquid. However, as the PCM melts and absorbs heat, the temperature difference between the PCM and the refrigerant decreases, so the outlet temperature increases with time. Thus, when the amount of refrigerant subcooling at the outlet is 5ºC, the refrigerant flow will stop, and HTF will begin to flow. The heat exchanger model used for the problem verification from Gong and Mujumdar's work

(1997) and the PCM condenser model, which is used on the next step, can be seen from the Figure 3.1 and Figure 3.2, respectively.

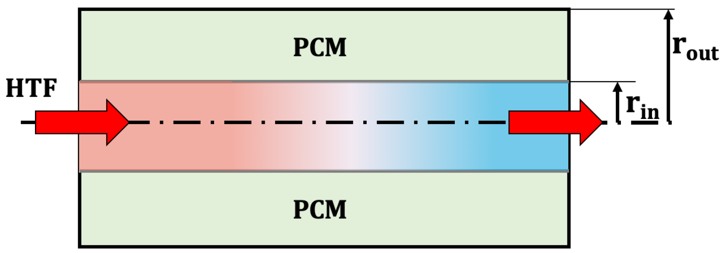

Figure 3.1 Schematic PCM heat exchanger model

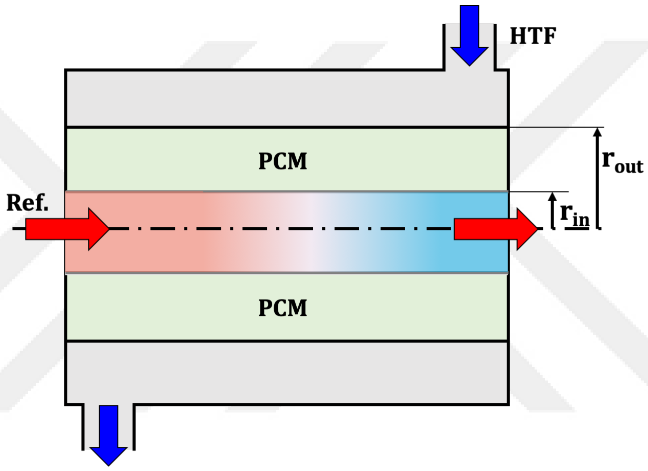

Figure 3.2 Schematic PCM condenser model

Properties of PCM are taken from RT28 HC by Rubitherm (Rubitherm.eu), and it is a kind of paraffin which is commonly used for heating and cooling applications between 0-65ºC temperature range. (Agyenim et al., 2010). The thermophysical properties of PCM are given in Table 3.1. For the PCM condenser problem, the refrigerant is chosen to be R134a, and HTF is water.

Table 3.1 Thermophysical properties of PCM (Rubitherm.eu)

Property	**PCM RT28HC**
Thermal Conductivity, W/mK	0.2 (for both phases)
Specific Heat, J/kgK	2000
Density, kg/m^3	770 (liquid), 880 (solid)
Latent Heat of Fusion, kJ/kg	250

3.2 Mathematical Formulation

The suggested mathematical model in this study is a condenser with a PCM layer between the inner and outer tubes where refrigerant and HTF flow, respectively. From inside to outside, each different layer of the condenser as refrigerant, PCM, and HTF is divided by a specified number of control volumes, which can be seen from Figure 3.3. Regions, where refrigerant and HTF flow is calculated, are modeled as only one dimensional as axial, whereas the PCM region is considered as two dimensional in both axial and radial direction.

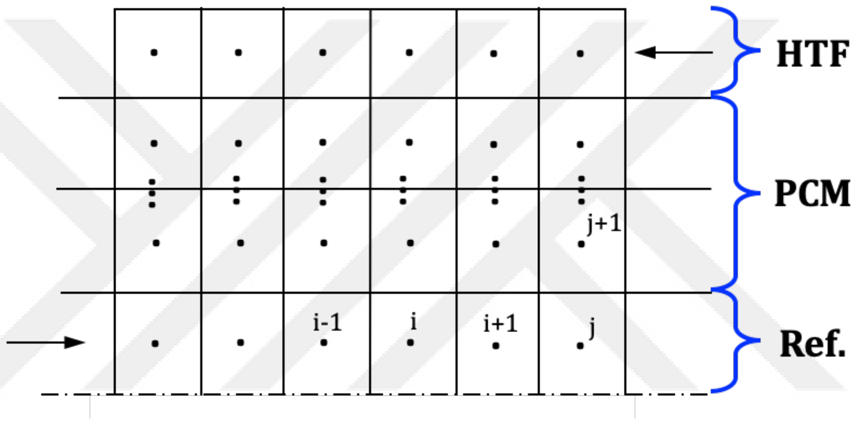

Figure 3.3 PCM condenser control volumes illustration

Mathematical modeling of the heat exchanger with the latent heat storage can be made using several approaches about conduction or natural convection inclusion or about the heat transfer coefficient calculation. The condenser model with PCM is evaluated according to the following conditions,

- Thermal conductivity is calculated through a harmonic mean values approach by Patankar (1980), and the conduction inside the PCM in both radial and axial direction is taken into consideration.
- Natural convection, when the melted PCM takes place, is neglected.
- PCM has stable thermophysical properties that are constant for the liquid and solid-state, separately.
- Thermal resistance between the tubes is neglected, and the outer surface of the condenser is assumed to be adiabatic.

- The heat transfer coefficient is taken as the refrigerant convective heat transfer during the charging process and HTF convective heat transfer coefficient during the discharge process, and it is calculated for each time step also depending on the location.
- Governing equations for both of the fluid flows are solved for the incompressible, Newtonian fluid in steady and transient forms.
- Axial heat conduction inside the refrigerant and HTF is neglected.

The energy equation for the refrigerant side can be written as previously described in Section 2.2 and Equation 2.3 for the solution of both condensing flow with PCM melting during the charging period and single-phase HTF flow with PCM solidification during the discharge period. The governing equations for the fluid flow will remain the same as in the first case with a double pipe condenser model.

For the PCM side, since the natural convection is neglected, dominant heat transfer will be via conduction inside the PCM layer except for the convection between the fluid flow at the boundaries of the middle tube with PCM. The energy equation for conduction-driven phase change should be solved and can be shown as below;

Energy:

$$\frac{\partial(\rho h)}{\partial t}+\frac{\partial(\rho uh)}{\partial z}+\frac{\partial(\rho vh)}{\partial y}=\frac{\partial}{\partial z}\left(k\frac{\partial T}{\partial z}\right)+\frac{\partial}{\partial y}\left(k\frac{\partial T}{\partial y}\right) \tag{3.1}$$

In this equation, PCM velocity in both directions *z*- and *y*- will be neglected. The discretization of the equation will be explained in detail in Section 3.3.

For the calculation method of enthalpy for both single-phase and multi-phase PCM, the temperature transforming method by Cao and Faghri (1990) is used. In their study, they developed a new method for temperature based fixed grid solutions according to their work; phase transition is assumed to occur in a range rather than a single point. Enthalpy term is calculated related to the temperature, and sensible and latent terms are separated by a source term. Enthalpy equation according to their approach is given as,

Enthalpy:

$$H = H_{\text{ref}} + \int_{T_{\text{ref}}}^{T} (\rho c_p)\, dT + \rho \Delta H f \tag{3.2}$$

$$H = CT + S \tag{3.3}$$

In this equation, H_{ref} means the reference enthalpy value, which is chosen as a reference point for integration, and f represents the liquid fraction. The enthalpy equation will be integrated between the defined temperature range where the phase change of PCM takes place. Different phase zones and the range between them can be shown as in Figure 3.4, and the boundaries between regions can define as follows;

- Solid PCM zone, $T \leq T_m - dT_m$
- Mushy PCM zone, $T_m - dT_m < T < T_m + dT_m$
- Liquid PCM region $T_m + dT_m \leq T$

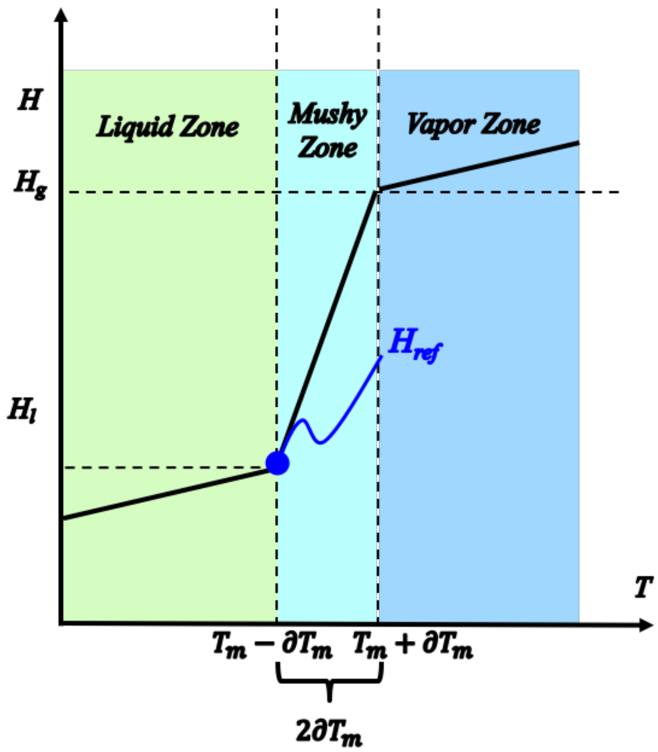

Figure 3.4 Temperature transforming method schematically

3.3 Numerical Solution

Generally, problems including PCM melting and solidification are called as 'Moving Boundary' problems because of the moving interface during phase transition from liquid to solid and vice versa (Fujii, 1995). There are different methods to solve numerical moving boundary problems. Formulations could differ from each other by means of grids of calculation. 'Fixed Grid' solutions deal with the fixed control volumes where the calculation is made. In this study, thanks to its easy implementation, the fixed grid solution is used, and grid size independency analysis is made to ensure the accuracy which is obtained by using the defined grid size, which will be mentioned in the later sections.

The most attractive and commonly used are the so-called enthalpy methods (Voller and Swaminathan, 1990). The major reason for that is that the method does not require explicit treatment of the conditions on the phase change boundary (Carslav and Jaeger 1959); there is no need for tracking the phase change boundary.

For the fixed grid solution in this work, one of the enthalpy methods, the temperature transforming method from Cao and Faghri (1990), is used. In this method, it is assumed that phase transition occurs in a temperature range, $dT_{m,}$ which is taken 0.01ºC in this study. Sensible and latent terms will be separated, and the equation below will be used for the enthalpy calculation, as previously shown in Equation 3.3. In this equation, the specific heat term, C is the sensible part, and the source term, S is the source term for the latent part, and these terms will be defined depending on the region that is separated from each other by the determined limits and can be shown as,

Specific Heat Term:

$$C = \begin{cases} (\rho c_p)_s & T \le T_m - \delta T_m \\ (\rho c_p)_m + \rho_l \dfrac{h_{sf}}{2\delta T_m} & T_m - \delta T_m < T < T_m + \delta T_m \\ (\rho c_p)_l & T \ge T_m + \delta T_m \end{cases} \tag{3.4}$$

Source Term:

$$S = \begin{cases} (\rho c_p)_l(\delta T_m - T_m) & T < T_m - \delta T_m \\ (\rho c_p)_m(\delta T_m - T_m) + \rho_l \dfrac{h_{sf}}{2} - \rho_l \dfrac{h_{sf}}{2\delta T_m} T_m & T_m - \delta T_m \le T \le T_m + \delta T_m \\ (\rho c_p)_s \delta T_m - (\rho c_p)_l T_m - \rho_l h_{sf} & T > T_m + \delta T_m \end{cases} \quad (3.5)$$

Subscripts *l, m,* and *s* refer to the liquid, mushy and solid phases, respectively. In the mushy zone, the mean value of the liquid and solid phase is calculated for the density and specific heat terms as follows,

$$(\rho c_p)_m = \frac{(\rho c_p)_l + (\rho c_p)_s}{2} \quad (3.6)$$

The solution method for refrigerant and HTF flow is the same as previously described in the first part of the study in the condenser model. In order to discretize the governing equations, a fully explicit scheme has been used. For the evaluation of the parameters at inlet and outlet interfaces, the upwind scheme is used.

In the second case, with phase change material applied to the condenser model, there is only a single fluid flow in the inner tube, and the outer tube is filled with PCM. After the outlet temperature reached the specified condition, which is defined as 5ºC superheat, then the refrigerant flow will stop, and HTF will begin flowing, and similarly, only one fluid flow at the outer tube and PCM layer will be solved. Enthalpy based method, which is one of the most common approaches (Fujii, 1995), is used, and the advantage of this method is that the solution is easily tractable and simply one energy equation similar to the single-phase can be used (Lacroix, 1993). Discretized equations for enthalpy are solved with Tri-Diagonal Matrix Algorithm, and for the temperature, the SIS algorithm is used.

At the inlet of the tubes where fluid flow occurs, equations depend on the inlet condition, which is constant inlet temperature and the enthalpy is calculated through energy balance between each grid.

At each time step, the solution algorithm first initialized, and guess values are assigned to the corresponding variables. Then, step-by-step first local thermophysical properties are evaluated, and the heat transfer coefficient and pressure drop are calculated through the convective heat transfer coefficient and friction factor, respectively. On the next step, specific heat and source term also conductivity term is calculated for the PCM side by Cao and Fagri's method (1990). Enthalpy can be calculated from these terms for the PCM layer, and the fluid layer enthalpy equation from the first part of this study is solved. The set of those equations are solved for each control volume iteratively until the defined convergence is achieved. Convergence criteria are defined as 10^{-6} as the previous case. If the solution converges, then energy balance is calculated between the fluid flow and the PCM layer. Storing or releasing the amount of energy by PCM should be equal to the enthalpy difference in either refrigerant or HTF. After each time step, the defined periodical basis boundary between solid and liquid zones inside the PCM is evaluated by means of melting temperature and local temperature distribution. The flow chart of the solution algorithm is shown in Figure 3.5.

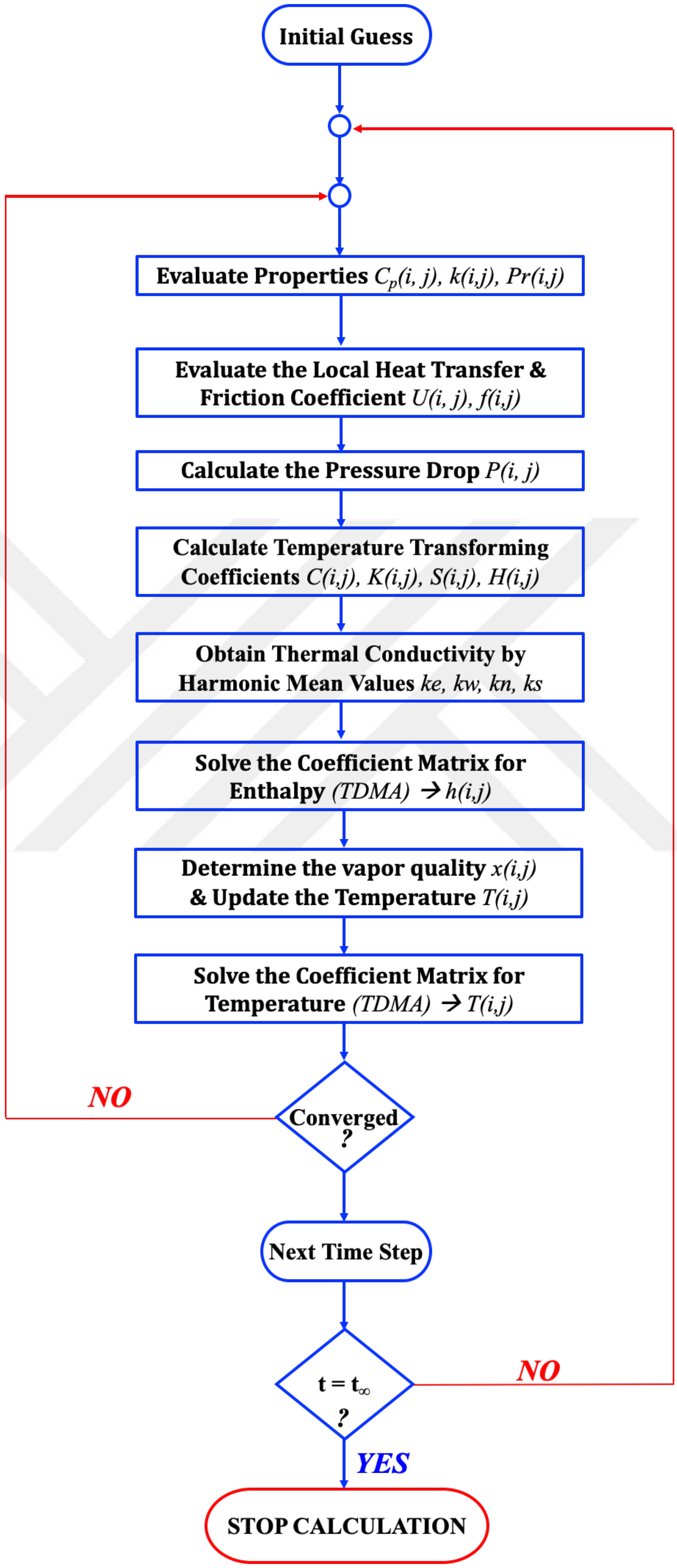

Figure 3.5 PCM condenser numerical solution flow chart

3.4 Verification

For the validation of the PCM Condenser problem, the first double pipe heat exchanger with a similar geometry is modeled and compared with experimental data from Gong and Mujumdar's work (1997). In their study, they have modeled a shell and tube heat exchanger with PCM. The validation of their problem is made by an overall energy balance for each time step by comparing the stored enthalpy of PCM and heat loss from HTF in the charging mode. Energy balance has never exceeded % 0.1, and for the validation of this part of the study, their charging cycle case is used. PCM and HTF properties with operating conditions are stated in Table 3.2 and 3.3. The PCM used in their study was a LiF 80.5%, and CaF2 19.5% mixture, and HTF is a mixture of He/Xe of which properties are taken at 627ºC.

Table 3.2 Validation problem PCM and HTF properties (Gong & Mujumdar, 1997)

Property	***PCM***	***HTF***
Thermal Conductivity, k_l (W/mK)	1.7	0.133
Thermal Conductivity, k_s (W/mK)	3.8	-
Specific Heat, *Cp* (J/kgK)	1770 (both phases)	502.2
Density, ρ_l & ρ_a (kg/m^3)	770 (liquid), 880 (solid)	1862
Latent Heat of Fusion, h_{fs} (kJ/kg)	816	-
Prandtl, Pr (-)	-	0.24
Melting Temperature, T_m (ºC)	767	-
Dynamic Viscosity, μ (kg/ms)	-	5.982 x 10^{-5}

The developed numerical algorithm is used to obtain results. Similar to the previously described, enthalpy of PCM are evaluated using temperature transforming method, and for the HTF side energy equation in enthalpy form is used, and the discretized equation is solved with Tri Diagonal Matrix Algorithm (TDMA). After enthalpy values in the entire domain are evaluated, the temperature is updated accordingly. Time parameters and geometric properties of the heat exchanger are taken as exactly the same as the chosen problem by Gong and Mujumdar (1997).

Table 3.3 Validation problem characteristics (Gong & Mujumdar, 1997)

Property	***Value***
Heat Exchanger Length, L (m)	1.5
Total Time, t (s)	17000
Initial Temperature, T_0 (ºC)	550
HTF Inlet Temperature, $T_{in, HTF}$ (ºC)	817
Time Step, Δt (s)	2
Inner Tube Radius, r_i (m)	0.0125
Outet Tube Radius, r_o (m)	0.025
HTF Velocity, V_{HTF} (m/s)	15
Heat Transfer Coefficient, U (W/m^{2}K)	89.16

In order to determine the grid size and time step to be used in the second part of the study for the PCM condenser model, mesh and time-step independency analyses are conducted.

As a result, 0.01 s for time step and 150 x 30 grid size are chosen for the next section of this study. Validation results are given by the outlet temperature of the HTF with time in Figure 3.6.

In Figure 3.6, outlet temperature values of the HTF is taken from the Gong and Mujumdar's work (1997); data is given for a limited time period starting from 740 *s*. It was seen that the difference between the Gong and Mujumdar's (1997) results and the developed numerical analysis results is 0.29%, and it shows good consistency. Thus, it can be concluded with this analysis that the PCM solution method developed for the PCM condenser problem can be used.

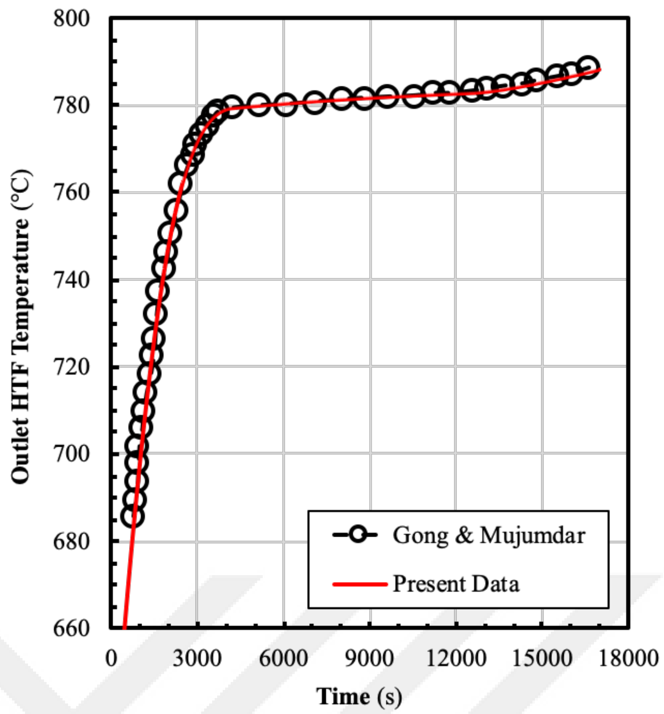

Figure 3.6 HTF outlet temperature comparison for validation (Gong & Mujumdar, 1997)

3.5 Results for PCM Condenser

After checking the validity, numerical calculations were conducted. Chosen parameters for the problem and refrigerant properties are given in Table 3.4. PCM used in the problem has thermal properties, as expressed in Section 3.1.

The problem is built according to the scenario explained below;

- At the initial state, the refrigerant inside the inner tube, HTF inside the outer tube, and the PCM layer between them is at 15ºC, the system was considered at a constant uniform temperature, which is lower than both PCM melting temperature and refrigerant R134a condensation temperature.
- As the superheated vapor refrigerant flow begins at 80ºC, HTF flow does not exist, and there is no heat transfer from PCM to HTF. PCM begins absorbing heat from the refrigerant, of which temperature decreases until the condensation temperature.

- When PCM reaches its melting temperature, it begins to liquefy, and a boundary between the solid and liquid PCM takes place.
- The fully condensed refrigerant then changes its state to sub-cooled or compressed liquid as it rejects its heat to the PCM and exits the condenser.
- HTF flow begins when the outlet temperature of the refrigerant has 5ºC subcooling.

Table 3.4 PCM condenser problem characteristics

Property	***Value***
Heat Exchanger Length, L (m)	5
Inner Diameter, D_i (m)	6
PCM Diameter, D_{PCM} (m)	8
Outer Diameter, D_o (m)	24
Initial Temperature, T_0 (ºC)	15
Refrigerant Inlet Temperature, $T_{ref,in}$ (ºC)	80
Refrigerant Saturation Temperature, T_{sat} (ºC)	45
HTF Inlet Temperature, $T_{HTF,in}$ (ºC)	15
Time Step, Δt (s)	0.01
Grid Size, z x r	150 x 30
Refrigerant Mass Flow Rate, $\dot{m}_{ref}$(kg/s)	0.5 x 10^{-2}
HTF Mass Flow Rate, $\dot{m}_{HTF}$ (kg/s)	0.1

3.5.1 Effect of mass flux on PCM condenser

Three cases are studied in these results in order to see the effect of different refrigerant mass flow rate. In 3 different cases, refrigerant mass flow rates are 2.5 x 10^{-2} kg/s, 12.5 x 10^{-2} kg/s and 0.5 x 10^{-2} kg/s, respectively. The temperature profile cannot reach steady-state conditions due to the moving boundary between two-phases within PCM. Thus, it is thought to have the results at different times to observe the phase transition of both PCM and refrigerant. The temperature variation of the condensing refrigerant R134a is given in Figure 3.7. Results are obtained for the aforementioned three cases and can be seen in Figure 3.7a, 3.7b, and 3.7c. Time periods for obtaining the results are varying according to the change in the temperature.

During the charging process of the case I, at the initial times, heat is slowly transferred to the PCM as the refrigerant flows horizontally inside the tube. PCM temperature keeps rising until it is reached to the melting temperature. Absorbed heat by the paraffin PCM equals the total enthalpy change in the refrigerant. As the PCM transfers energy vertically, different temperature profiles begin to form at different locations. After melting, not only the conduction but also the convection affects the upper points of the region. Since the temperature difference is decreased with time, the increase rate of the temperature also slowed gradually.

In case II, the mass flow rate of the refrigerant is five times bigger than the previous case. The bigger volume of refrigerant has more energy to transfer, and heat transfer at the same instance is bigger, which leads to a more uniform and slow-changing temperature distribution since there is a more uniform temperature inside the inner tube and temperature values on the wall show less variability.

For case III, the temperature inside the PCM domain is less compared to the other two cases for the beginning. The reason for that is the refrigerant mass flow rate is lower than the other cases. For all the cases, at the inlet of the PCM condenser, thermal conductivity is high, and the temperature difference between refrigerant and PCM domain is at its maximum. As the flow and heat transfer from each other takes place, the gradient of temperature gets smaller, and consequently, heat transfer becomes slower and smaller.

From Figure 3.7, in the first case, the refrigerant condenses in a relatively short time. After 7.5 *s*, the refrigerant temperature goes higher than saturation. Since the heat transfer is higher when the fluid flow is multi-phase, accordingly, melting occurs faster. On the other hand, in Case II, the mass flow rate of the refrigerant has the biggest value. Thus, even though the refrigerant temperature drop is faster alongside the condenser, the temperature cannot fall to the condensation temperature due to the larger volume of refrigerant. For the last case, since the volume of the refrigerant is smallest, the temperature can drop until the subcooling region and condensation takes the longest period. As time passes, two-phase region grows, which leads to a higher heat transfer.

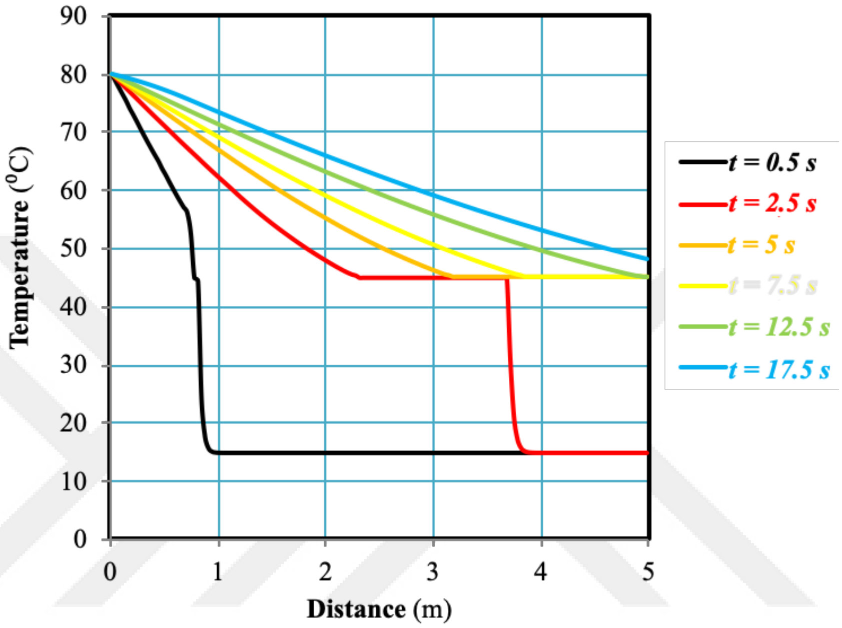

a. Case I, $\dot{m}_{REF}$ = 2.5 x 10^{-2} kg/s

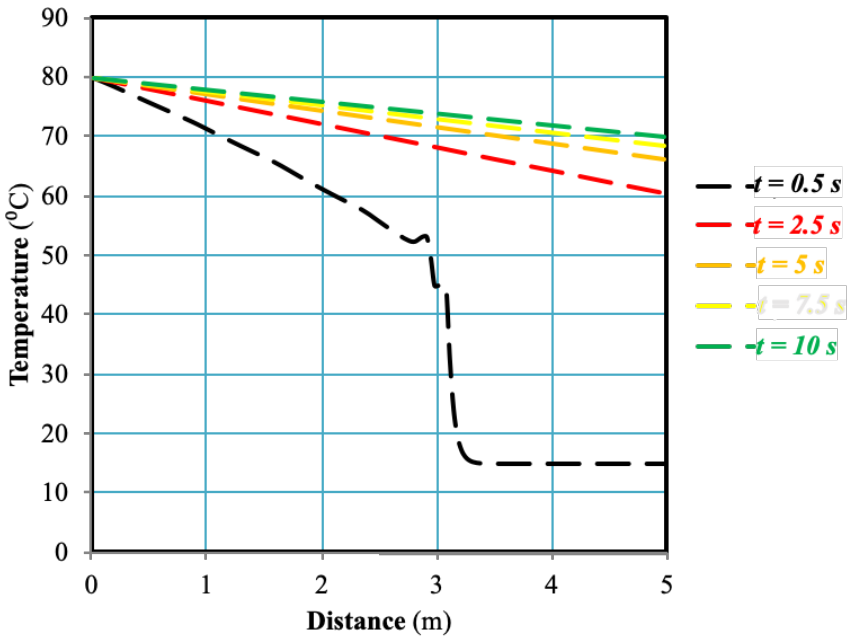

b. Case II, $\dot{m}_{REF}$ = 12.5 x 10^{-2} kg/s

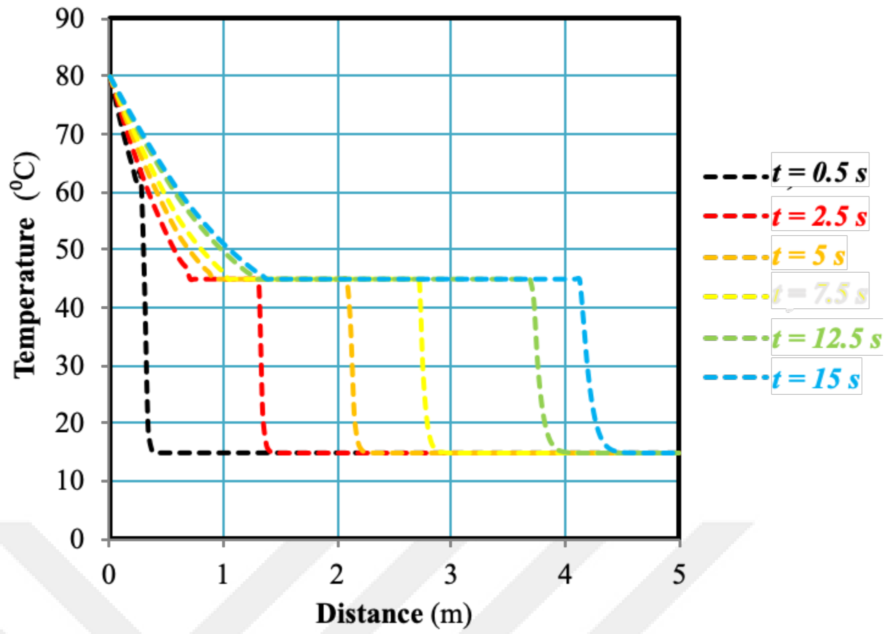

c. Case III, $\dot{m}_{REF} = 0.5 \times 10^{-2}$ kg/s

Figure 3.7 Temperature variation of the refrigerant at different instances

CHAPTER FOUR
CONCLUSION

The numerical model of a PCM condenser is developed to be used in heat pump systems using waste-water heat recovery. Temperature values, refrigerant, and geometry of the condenser are chosen according to this aim.

At first, a double-pipe condenser model is developed with refrigerant inside the inner tube and HTF flowing in the outer tube. Then as the second part of the study, the PCM condenser model is studied by adding extra PCM layer between the tubes from the previous condenser model.

The accuracy of the solution algorithms used in the double pipe condenser and PCM condenser is validated through numerical and experimental data from the published literature.

According to the results, it can be concluded that,

- A relatively simple numerical model is developed, and it can be used for the heat exchangers with a multi-phase flow such as condensers and evaporators.
- Spontaneous phase transitions of condensation and melting are modeled, and temperature distribution is obtained logically at expected values using the developed model.
- The developed PCM condenser model can be used in systems where the heat removed from the condenser is recovered and stored in PCM. The next regeneration need for the melted PCM can be supplied by the relatively colder waste-water from the residential heat pump systems.

REFERENCES

Agyenim, F., Hewitt N., Eames, P., & Smyth M. (2010). A review of materials, heat transfer and phase change problem formulation for latent heat thermal energy storage systems (LHTESS). *Renewable and Sustainable Energy Reviews, 14,* 615–628.

ASHRAE, (1985). *ASHRAE handbook 1985 fundamentals volume.* Atlanta: ASHRAE.

Baek, N. C., Shin, U. C., & Yoon, J. H. (2005). A study on the design and analysis of a heat pump heating system using wastewater as a heat source. *Solar Energy, 78,* 427–440.

Bivens, D. B., & Yokozeki, A. (1994). Heat transfer coefficient and transport properties for alternative refrigerants. *International Refrigeration Conference, Purdue, Indiana,* 299–304.

Van de Bor, J. H., Infante Ferreira, C. A., & Kiss, A. A. (2015). Low grade waste heat recovery using heat pumps and power cycles, *Energy, 89,* 1-10.

Boyko, L. D. & Kruzhilin, G. N. (1969). Heat transfer and hydraulic resistance during condensation of steam in a horizontal tube and in a bundle of tubes. *International Journal of Heat and Mass Transfer, 10,* 361-373.

Cao, Y., & Faghri, A. (1990). A numerical analysis of phase-change problems including natural convection. *Journal of Heat Transfer, 112*(3), 812–816.

Cavallini, A., Censi, G., Del Col, D., Doretti, L., Longo, G.A., & Rossetto, L. (2001). Experimental investigation on condensation heat transfer and pressure drop of new HFC refrigerants (R134a, R125, R32, R410A, R236ea) in a horizontal smooth tube. *International Journal of Refrigeration, 24*, 73-87.

Chao, S., Yiqiang, J., Yang, Y., Shiming, D., & Xinlei, W. (2012). A field study of a wastewater source heat pump for domestic hot water heating. *Building Services Engineering Research and Technology, 34*(4), 433–448.

Chen, H. & Lee, W. L. (2010). Combined space cooling and water heating system for Hong Kong residences. *Energy and Buildings ,42*, 243–250.

Chen, W., Liang, S., Guo, Y., Cheng, K., Gui, X., & Tang, D. (2013). Investigation on the thermal performance and optimization of a heat pump water heater assisted by shower waste water. *Energy and Buildings, 64,* 172–181.

Churchill, S. W. (1977). Frictional equation spans all fluid flow regimes. *Chemical Engineering, 114,* 91-92.

Daviran, D., Kasaeian, A., Golzari, S., Mahian, O., Nasirivatan, S., & Wongwises, S. (2017). A comparative study on the performance of HFO-1234yf and HFC-134a as an alternative in automotive air conditioning systems. *Applied Thermal Engineering, 110,* 1091–1100.

Dobson, M. K., & Chato, J. C. (1998). Condensation in smooth horizontal tubes. *Journal of Heat Transfer, 120*, 193–213.

Dupont, T., Fairweather, G., & Johnson, J. P. (1974). Three-level Galerkin methods for parabolic equations, *SIAM Journal on Numerical Analysis, 11,* 392–410.

Ekren, O., Araz, M., Hepbasli, A., Biyik, E., & Gunerhan, H. (2016). Design aspects and experimental performance test of a wastewater heat pump for the mediterranean climate. *Journal of Clean Energy Technologies, 4*(5), 371-374.

Escanes, F., Pérez-Segarra, C. D., & Oliva, A. (1995). Thermal and fluid-dynamic behaviour of double-pipe condensers and evaporators—a numerical study.

International Journal of Numerical Methods for Heat & Fluid Flow, 5(9), 781 – 795.

EU, *EU Regulation No 517/2014 of the European Parliament and of the council on fluorinated greenhouse gases and repealing Regulation (EC) No 842/2006,* Retrieved July 14, 2020, from https://ec.europa.eu/clima/policies/f-gas.

Fayssal, I., & Moukalled, F. (2012). A new numerical approach for predicting the two-phase flow of refrigerants during evaporation and condensation. *Numerical Heat Transfer, Part B: Fundamentals, 62*(5), 341-369.

Fujii, T. (1995). Enhancement to condensing heat transfer—new developments. *Journal of Enhanced Heat Transfer, 2,* 127–137.

Garcia-Valladares, O., Perez-Segarra, C. D., Rigola, J., & Oliva, A. (1998). Detailed numerical simulation of condensers and evaporators using pure and mixed refrigerants. *International Compressor Engineering Conference,* 839-844.

García-Valladares, O. (2003). Review of in-tube condensation heat transfer correlations for smooth and microfin tubes, *Heat Transfer Engineering, 24*(4), 6-24.

Garcia-Valladares, O., Perez-Segarra, C. D., & Rigola, J. (2004). Numerical simulation of double-pipe condensers and evaporators. *International Journal of Refrigeration, 27,* 656–670.

Gong, Z. X., & Mujumdar, A. S. (1996). Cyclic heat transfer in a novel storage unit of multiple phase change materials. *Applied Thermal Engineering 16*(10), 807-815.

Gong, Z. X., & Mujumdar, A. S. (1997). Finite-element analysis of cyclic heat transfer in a shell-and-tube latent heat energy storage exchanger. *Applied Thermal Engineering, 17*(6), 583-591.

Gu, Y., Wang, T., Liu, W., & Ma F. (2014). Energy-saving analysis and heat transfer performance of wastewater source heat pump. *Applied Mechanics and Materials, 694,* 211-217.

Hepbasli, A., Biyik, E., Ekren, O., Gunerhan, H., Araz, M. (2014). A key review of wastewater source heat pump (WWSHP) systems. *Energy Conversion and Management, 88,* 700–722.

Hosseini, M. J., Rahimi, M., & Bahrampoury, R. (2014). Experimental and computational evolution of a shell and tube heat exchanger as a PCM thermal storage system. *International Communications in Heat and Mass Transfer, 50*, 128–136.

Jaster, H., & Kosky, P. G. (1976). Condensation heat transfer in a mixed flow regime. *International Journal of Heat and Mass Transfer, 19,* 95-99.

JSME Data Book, (1983). *Thermalphysical properties of fluids.* Japan: JSME.

Kandlikar, S. G. (Ed.) (1999). *Handbook of phase change: boiling and condensation.* Philadelphia: Taylor & Francis.

Linde-gas, R1234yf – Opteon® YF brochure. Retrieved November 9, 2019, from http://www.linde-gas.com/en/products_and_supply/refrigerants/hfo_refrigerants/index.html

Lockhart, R. W., & Martinelli, R. C. (1949). Proposed corelation of data for isothermal two-phase, two-component flow in pipes. *Chemical Engineering Progress, 45*(1), 39-48.

Long, J. Y., & Zhu, D. S. (2008). Numerical and experimental study on heat pump water heater with PCM for thermal storage. *Energy and Buildings 40,* 666–672.

Maaraoui, S., Clodic, D., & Dalicieux, P. (2012). Heat pump with a condenser including solid-liquid phase change material. *International Refrigeration and Air Conditioning Conference,* 1194.

McNabola, A., & Shields, K. (2013). Efficient drain water heat recovery in horizontal domestic shower drains. *Energy and Buildings, 59,* 44–49.

Nyers, J. (2016). COP and economic analysis of the heat recovery from waste water using heat pumps. *Acta Polytechnica Hungarica, 13*(5), 135-154.

Ozisik, N. (1994). *Finite difference methods. Heat Transfer Book, 2nd Edition.* New York: CRC Press.

Parry, A. J., Eames, P. C, & Agyenim, F. B. (2014). Modeling of thermal energy storage shell and tube heat exchanger. *Heat Transfer Engineering, 35*(1), 1-14.

Patankar, S. (1980). *Numerical heat transfer and fluid flow.* New York: McGraw-Hill.

Pettit, N. B. O. L., Willatzen, M., & Ploug-Sørensen, L. (1998). A general dynamic simulation model for evaporators and condensers in refrigeration. Part II: Simulation and control of an evaporator. *International Journal of Refrigeration, 21*(5), 404–414.

Prather, D. (2017). *Why r-32 may be the refrigerant of the future.* Retrieved November 9, 2019, from https://www.achrnews.com/articles/134215-why-r-32-may-be-the-refrigerant-of-the-future.

Qiao, Y., Mallow, A., Muehlbauer, J., Hwang, Y., Ling, J., Aute, V., Radermacher, R., & Gluesenkamp, K. R. (2018). Experimental study on portable air-conditioning system with enhanced pcm condenser. *17th International Refrigeration and Air Conditioning Conference at Purdue,* 2483.

Qiu, F., Li, B., & Xu, T. (2019). Experimental investigations on the thermal performance of a domestic condensing heat recovery air-conditioner. *Advances in Mechanical Engineering, 11*(2), 1–14.

Ramadan, M., Lemenand, T., & Khaled, M. (2016). Recovering heat from hot drain water—Experimental evaluation, parametric analysis and new calculation procedure. *Energy and Buildings, 128,* 575–582.

REFPROP v.6.01. *NIST thermodynamic properties of refrigerants and refrigerant mixtures database* (1998). Standard Reference Data Program, USA.

Rigola, J., Morales, S., Gustavo, R., & Segarra C. D. P. (2004). Analysis of two-phase flow in double-pipe condensers and evaporators with special emphasis on transition zones: numerical model and experimental comparison. *International Refrigeration and Air Conditioning Conference,* 658.

Rohsenow, W. M. (Ed.), Hartnett, J. P. (Ed.), & Cho, Y. I. (Ed.). (1998). *Handbook of heat transfer. 3rd edition, Chapter 14.* New York: McGraw-Hill.

Rösler, F. & Brüggemann, D. (2011). Shell-and-tube type latent heat thermal energy storage: numerical analysis and comparison with experiments. *Heat Mass Transfer, 47,* 1027–1033.

Rubitherm.eu. RT 28HC Datasheet. Retrieved June 10, 2020, from https://www.rubitherm.eu/media/products/datasheets/Techdata_RT28HC_EN_06082018.PDF

Ruiz, M, Rigola, J., Pérez-Segarra, C. D., & García-Valladares, O. (2009). Numerical analysis of two-phase flow in condensers and evaporators with special emphasis on single-phase/two-phase transition zones. *Applied Thermal Engineering, 29,* 1032–1042.

Sari, A., & Kaygusuz, A. (2001). Thermal energy storage system using stearic acid as a phase change material. *Solar Energy, 71*(6), 365–376.

Seddegh, S., Wang, X., & Henderson, A. D. (2016). A comparative study of thermal behaviour of a horizontal and vertical shell-and-tube energy storage using phase change materials. *Applied Thermal Engineering 93,* 348–358.

Shah, M. M. (1979). A general correlation for heat transfer during film condensation inside pipes. *International Journal of Heat Mass Transfer 22,* 547-556.

Shao, D. W., & Granryd E. G. (2000). Flow pattern, heat transfer and pressure drop in flow condensation. Part i: pure and azeotropic refrigerants. *HVAC&R Research, 6*(2), 175–195.

Soliman, H. M. (1982). On the annular-to-wavy flow pattern transition during condensation inside horizontal tubes. *The Canadian Journal of Chemical Engıneering, 60,* 475-481.

Stephan, K. (1992), *Heat transfer in condensation and boiling.* New York: Springer.

Tandon, T. N., Varma, H. K., & Gupta, C. P. (1995). Heat transfer during forced convection condensation inside horizontal tube. *International Journal of Refrigeration, 18*(3), 210–214.

Tang, L., Ohadi, M. M., & Johnson A. T. (2000). Flow condensation in smooth and microfin tubes with hcfc-22, hfc-134a, and hfc-410 refrigerants. Part II: Design equations. *Journal of Enhanced Heat Transfer, 7,* 311–325.

Voller V. R., & Prakash C. (1987). A fixed grid numerical modelling methodology for convection-diffusion mushy region phase change problems. *International Journal of Heat Mass Transfer, 30,* 1709–1719.

Voller, V. R., & Swaminathan, C. R. (1990). Fixed grid techniques for phase change problems: A review. *International Journal for Numerical Methods in Engineering, 30,* 875-898.

Wallis, G. B. (1969). *One-dimensional two-phase flow*. New York: McGraw-Hill Book Company.

Wallis, G. B. (1982). Review—Theoretical models of gas-liquid flows. *Journal of Fluids Engineering, 104,* 279-283.

Wang, C. C., & Liao, N. S. (1989). Transient response of a double-pipe condenser to change of coolant flowrate. *International Communications in Heat and Mass Transfer, 16,* 325-334.

Willatzen, M., Pettit, N. B. O. L., & Ploug-Sørensen, L. (1998). A general dynamic simulation model for evaporators and condensers in refrigeration. Part I: moving-boundary formulation of two-phase flows with heat exchange. *International Journal of Refrigeration, 21*(5), 398–403.

Zalba, B., Marin, J. M., Cabeza, L. F., & Mehling, H. (2003). Review on thermal energy storage with phase change: materials, heat transfer analysis and applications. *Applied Thermal Engineering, 23,* 251–283.

Zhang, X., Yu, S., Yu, M., & Lin, Y. (2011). Experimental research on condensing heat recovery using phase change material. *Applied Thermal Engineering 31,* 3736-3740.

Zienkiewicz, O. C., & Taylor, R. L. (1989). *The finite element method.* London: McGraw-Hill.

APPENDICES

SYMBOLS

A	Heat transfer area (m^2)
A_c	Cross sectional area (m^2)
c_p	Specific heat (kJ/kgK)
dT_m	Mushy zone temperature range (°C)
D	Diameter (m)
f	Darcy friction factor (-)
G	Mass flux (kg/m^2s)
h	Enthalpy (kJ/kg)
i	Grid parameter in axial direction (-)
j	Grid parameter in radial direction (-)
H	Enthalpy term multiplied with mass (kJ)
h_{conv}	Convective heat transfer coefficient (W/m^2K)
k	Thermal conductivity (W/mK)
m	Mass (kg)
$\dot{m}$	Mass flow rate (kg/s)
q''	Heat flux (W/m^2)
P	Perimeter (m)
p	Pressure (kPa)
r	Radius (m)
Pr	Prandtl (-)
Re	Reynolds number $(\rho u D/\mu)$
S	Source term
t	Time (s)
T	Temperature (°C)
u	Velocity in axial direction (m/s)
v	Velocity in radial direction (m/s)
U_{TP}	Two-phase heat transfer coefficient (W/m^2K)
x	Vapor quality (-)
z	Axial position parameter (-)

y	Radial position parameter (-)

Greek symbols

ρ	Density (kg/m^3)
ε^*/D	Relative roughness (-)
ε	Convergence criteria (-)
ϕ	General dependent parameter (-)
μ	Viscosity (kg/ms)
Δt	Time-step size (s)
Δz	Control volume distance (m)
τ	Shear stress (kg/ms^2)

Subscripts

ref	Refrigerant
m	Mushy zone, Mean
red	Reduced
in	Inlet, Inner
out	Outlet, Outer
HTF	Heat transfer fluid
g	Gas
l	Liquid
TP	Two-phase
c	Cross-sectional